

Thank you very much for your interest in our paper. As you noted, this study aims to make a significant contribution to determining the reliability of GCMs in climate prediction and impact assessment. Previous bias correction studies have primarily focused on selecting the appropriate method based on performance alone; however, this approach has limitations due to the uncertainties arising from various factors. Our research proposes a comprehensive index that integrates uncertainty quantification with performance evaluation when selecting bias correction methods. This approach provides an opportunity to further enhance the reliability of climate models. Specifically, we expect that the results of this study will be effectively used in the process of selecting GCMs and evaluating the various methods applied in the models, ultimately aiding in the choice of the most suitable approach. Once again, we sincerely appreciate your interest and valuable feedback. Now, I would like to address your comments.

Comment 1

L50: What do the authors mean by “which has reduced difference between GCM simulations and observed precipitation? Do the authors mean uncertainty/error in GCMs relative to the observed?”

Answer

We thank the reviewer for raising this important point. In the original sentence, “reduced the difference between GCM simulations and observed precipitation,” we intended to convey that the bias correction methods decrease the systematic errors namely, the bias present in raw GCM outputs when compared to observed (or reference) precipitation data. Raw GCM simulations often exhibit significant discrepancies from observations due to inherent model limitations and incomplete representations of key physical processes. Therefore, many studies apply various bias correction techniques (e.g., quantile mapping methods) to adjust the raw simulations so that they align more closely with observed precipitation, thereby reducing error metrics such as RMSE or MAE. We have clarified this point in the revised manuscript to emphasize that “reduced difference” refers to the decrease in systematic bias/error rather than a reduction in model uncertainty. In addition, we have revised the sentence to clearly express its meaning as follows:

Many studies have developed appropriate bias correction methods based on various theories, which have reduced the difference between raw GCM simulations and observed precipitation (Abdelmoaty and Papalexiou, 2023; Shanmugam et al., 2024; Rahimi et al., 2021).

Comment 2

L57: change “a recent study” to “recent studies” and remove “an”

Answer

Thank you for your comment. We acknowledge that there were some errors in writing the sentence.

Taking your comments into account, we have revised the sentence as follows:

To address these limitations, recent studies proposed an improved QM approach to reflect future non-stationary precipitation across all quantiles of historical precipitation (Rajulapati and Papalexiou, 2023; Cannon et al., 2015; Cannon, 2018; Song et al., 2022b).

Comment 3

L70: There is an abrupt deflection from the bias correction discussion to the MCDA in this paragraph disrupting the flow from the previous paragraph. Authors emphasized the need for selecting appropriate bias correction methods in L67 – 69 and abruptly jumped to GCMs performance evaluation and then again to bias correction. I suggest moving paragraph three to paragraph four and paragraph four to three. Authors should also add a brief importance of TOPSIS to the MCDA method and why it was chosen out of the many other MCDA methods. Nothing about the BMA method was also mentioned in any part of the introduction except at the last paragraph that it was used. While this information is always detailed in the methodology section, briefly introducing while they are used in the introduction section gives comprehensiveness to this section.

Answer

We have carefully considered the reviewer's suggestion regarding the change in paragraph order. However, in paragraph 3 we describe the reasons behind the implementation of existing bias correction methods for GCMs, their limitations, and the various approaches that have been proposed to overcome these shortcomings. In particular, the last sentence emphasizes that the improved QM techniques do not provide uniform results across all grids and points, thereby necessitating a robust evaluation framework for selecting the appropriate QM method. The following paragraph then naturally introduces the MCDA framework. Thus, we believe that the current structure, without any change in paragraph order, already maintains a sufficient logical flow and connectivity.

Nonetheless, to strengthen paragraphs 3 and 4, we have added the following passages regarding TOPSIS and BMA:

Technique for Order Preference by Similarity to Ideal Solution (TOPSIS) is effectively utilized in our study's MCDA framework by integrating multiple evaluation metrics and calculating the distance between each alternative and the ideal solution, thereby enabling clear and intuitive prioritization decisions.

Furthermore, Bayesian Model Averaging (BMA) plays a crucial role in quantifying the predictive uncertainty of multiple climate models and enhancing the reliability of the final predictions, which is why it has been employed as an indispensable tool in our integrated evaluation.

Comment 4

L79: This line in part shows the justification for this research. I suggest authors put all justification for the study in the second to the last or last paragraph of this section.

Answer

Thank you for your insightful comment. We have incorporated your suggestions by adding the following sentence to the introduction:

In light of the challenges outlined above, including discrepancies among bias correction methods, regional variability in precipitation distributions, and significant uncertainties in GCM outputs, there is a clear need for an integrated framework that evaluates the performance of various QM methods and quantifies their associated uncertainties.

Comment 5

L96: change “simulation” to “simulated” or change “simulation precipitation” to “precipitation simulation”

Answer

Thank you for your comment. We have revised the text as follows:

However, accurately identifying biases in **precipitation simulation** remains challenging due to the lack of comprehensive equations reflecting Earth's physical processes.

Comment 6

L121: Considering that there are many GCMs, why did the authors consider just 11 in their study?

Answer

The reason we used only 11 CMIP6 GCMs in this study is that applying QM methods requires extensive computational time. Generating bias-corrected results with three QM methods across 11 CMIP6 GCMs took more than six months. Nonetheless, we determined that using fewer than 10 GCMs would not adequately justify the study, which is why we employed 11 CMIP6 GCMs. We appreciate your understanding on this matter.

Comment 7

L122: mentioning temperature here is not necessary since the study doesn't consider temperature.

Answer

Thank you for your comment. We have removed the sentence from the main text in response to your suggestion.

Comment 8

L129: In table 1. I think the climate variables and the variant label columns are not necessary since only single ones were used. Mentioning it in the text is sufficient. Authors should consider including the full name of the institutions or any other information.

Answer

Thank you for your comment. In response, we have revised Table 1 and the text as follows:

Table 1. Information of CMIP6 GCMs in this study

Institution	Models	Resolution
Commonwealth scientific and industrial research organization/ Australia	ACCESS-CM2	$1.2^\circ \times 1.8^\circ$
	ACCESS-ESM1-5	$1.2^\circ \times 1.8^\circ$
Beijing Climate Center/China	BCC-CSM2-MR	$1.1^\circ \times 1.1^\circ$
Canadian Centre for Climate Modeling and Analysis/ Canada	CanESM5	$2.8^\circ \times 2.8^\circ$
National Center for Atmospheric Research	CESM2-WACCM	$0.9^\circ \times 1.3^\circ$
Euro-Mediterranean Center on Climate Change coupled climate model/ Italy	CMCC-CM2-SR5	$\sim 0.9^\circ$
	CMCC-ESM2	$0.9^\circ \times 1.25^\circ$
EC-Earth Climate Model Consortium/ EC-EARTH consortium	EC-Earth3-Veg-LR	$1.0^\circ \times 1.0^\circ$
National Oceanic and Atmospheric Administration/ United States	GFDL-ESM4	$1.4^\circ \times 1.4^\circ$
Institute for Numerical Mathematics/ Russia	INM-CM4-8	$\sim 0.9^\circ$
Institute Pierre Simon Laplace/ France	IPSL-CM6A-LR	$1.1^\circ \times 1.1^\circ$

Comment 9

L136: change “availability” to “purpose”

Answer

Thank you for your comment. We attempted to locate the term "availability" in L136, but it was not present. Please review it once again.

Comment 10

L146 – 148: were the historical GCMs corrected before comparison to the observed? If so, why was this done since many studies usually compare the raw GCMs first with the reference before bias correcting and then comparing the bias corrected with the reference. If otherwise, authors should rephrase the sentence.

Answer

Thank you for your comment. In this study, we compared the raw GCMs and the bias-corrected GCMs with the reference data. In particular, Figure 1 compares the bias-corrected GCMs and raw GCMs using Taylor diagrams.

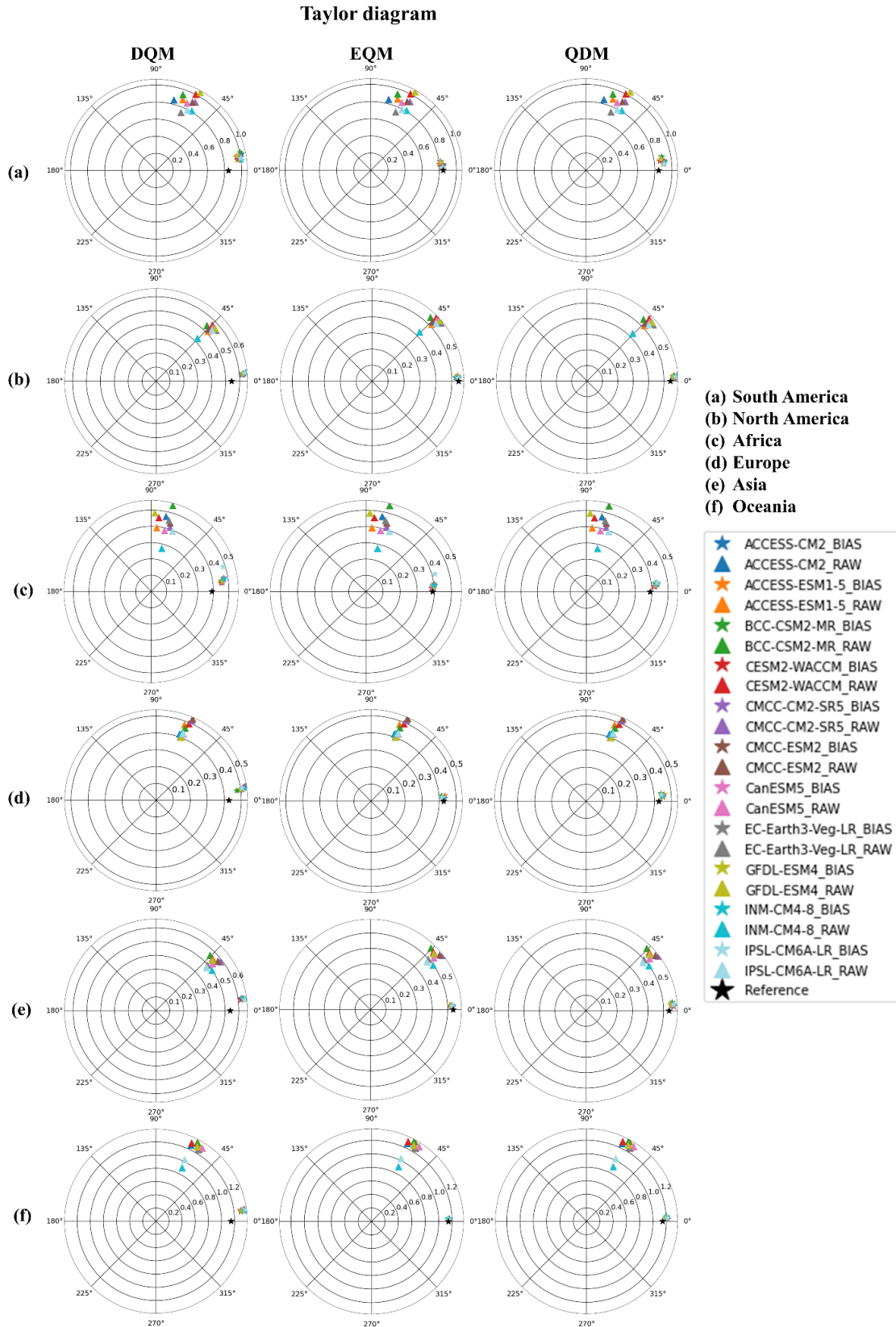


Figure 1. Comparison of raw and corrected daily precipitation on six continents using Taylor diagrams

Comment 11

L148: why was the “frequency-adaptation technique” further needed?.

Answer

Frequency-adaptation is used not only to adjust the magnitude of a climate variable but also the frequency of its events. Climate models, particularly for variables such as precipitation, often exhibit biases in both the intensity of precipitation and the number of precipitation days (i.e., the frequency) compared to observations. This technique adjusts the frequency of precipitation in the model output so that it more closely matches the observational data, thereby enhancing the realism of the overall distribution and the representation of extreme events. In addition, frequency adaptation is employed to address the issue that regional climate models often simulate a lower frequency of dry days than observed, which, if left uncorrected, would lead to a systematic wet bias in the bias-corrected precipitation. This technique randomly interpolates a portion of the excess dry-day cases to preserve the observed distribution of dry days and improve the overall accuracy of Quantile Mapping. The effectiveness of this approach has been demonstrated in Themeßl et al. (2011). For example, when correcting precipitation, if a model predicts too many light rain events or too few heavy rain events compared to reality, the frequency-adaptation technique adjusts these frequency differences. As a result, both the magnitude and the frequency of precipitation events are accurately represented, leading to more reliable climate predictions.

Comment 12

L187: The authors mentioned 10 metrics and again later mentioned 7 metrics. Table show 10 were used. Authors should correct this in text.

Answer

Thank you for your comment. In response to your suggestion, we have revised the sentence as follows:

Ten evaluation metrics used in this study are as follows: Root Mean Square Error (RMSE), Mean Absolute Error (MAE), Coefficient of Determination (R^2), Percent bias (Pbias), Nash-Sutcliffe Efficiency (NSE), Kling-Gupta Efficiency (KGE), Median Absolute Error (MdAE), Mean Squared Logarithmic Error (MSLE), Explained Variance Score (EVS), and Jensen-Shannon divergence (JS-D).

Comment 13

L187: The authors mentioned 10 metrics and again later mentioned 7 metrics. Table show 10 were used.

Authors should correct this in text.

Answer

Thank you for your comment. In response to your suggestion, we have revised the sentence as follows:

Ten evaluation metrics used in this study are as follows: Root Mean Square Error (RMSE), Mean Absolute Error (MAE), Coefficient of Determination (R^2), Percent bias (Pbias), Nash-Sutcliffe Efficiency (NSE), Kling-Gupta efficiency (KGE), Median Absolute Error (MdAE), Mean Squared Logarithmic Error (MSLE), Explained Variance Score (EVS), and Jensen-Shannon divergence (JS-D).

Comment 14

L206: GEV was not mentioned at all in the introduction section. A brief introduction about it and its usage should be introduced in the introduction section.

Answer

Thank you for your comment. In response, we have added the following sentence:

Furthermore, they compared the extreme precipitation of GCMs using the GEV distribution, which allows for more effective estimation of extreme precipitation, and demonstrated that the performance in estimating extreme precipitation varies according to different bias correction methods.

Comment 15

L291: The first sentence: “This study applied.....” is a repetition. It should be removed..

Answer

Thank you for your comment. In response to your suggestion, we have revised the sentence as follows:

A Taylor diagram was used to compare the bias-corrected and raw GCM precipitation with the observed data, and Figure 1 presents the results of applying the three QM methods to 11 CMIP6 GCMs.

Comment 16

L292: Authors mentioned that figure 1 show the before and after bias correction of the precipitation. There is no indication of the before and after correction in the figure. The figure seems to be showing either of them. Authors should clarify. Figure also shows there seems to be no any changes in the performances of some models based on the three BC methods in some regions. For example, in South America where there are no changes based on the BC methods for models between 45 - 90 o . What could be the reason for these?

Answer

Thank you for your comment. In Figure 1, the triangles represent the raw GCM precipitation, while the star symbols represent the bias-corrected GCM precipitation. Furthermore, the black star in Figure 1 denotes the reference data, and most of the bias-corrected GCM precipitation values closely match the reference data across all continents. The models located between 45° and 90° in South America, as you mentioned, represent the raw GCM precipitation. Therefore, all the Taylor diagrams in Figure 1 include both raw and bias-corrected GCM precipitation.

Comment 17

L320: This study.....This is not necessary. It can be removed.

Answer

Thank you for your comment. In response to your suggestion, we have revised the sentence as follows:

The spatial patterns of the evaluation metrics computed from the bias-corrected daily precipitation data of GCMs in South America are presented as shown in Figures 2 and S1.

Comment 18

L339: did authors meant North America here?

Answer

Thank you for your comment. We made some errors while drafting the text, and in response to your suggestion, we have revised the sentence as follows:

Figures 3 and S2 present the spatial patterns of these evaluation metrics, calculated for daily precipitation from the bias-corrected GCMs in North America.

We utilized supplementary materials to present the results of all evaluation metrics for each continent. Accordingly, the main text explains the outcomes for all 10 evaluation metrics. To further demonstrate that the diversity and computations described in the main text were indeed carried out, we provided various indices. Moreover, the influence of factors such as geographic features (e.g., deserts) on the performance of bias correction methods across regions was primarily discussed in the discussion section with respect to the observations.

Comment 19

L339: did authors meant North America here?

Answer

Thank you for your comment. In response to your suggestion, we have revised the caption for Figure 7 as follows:

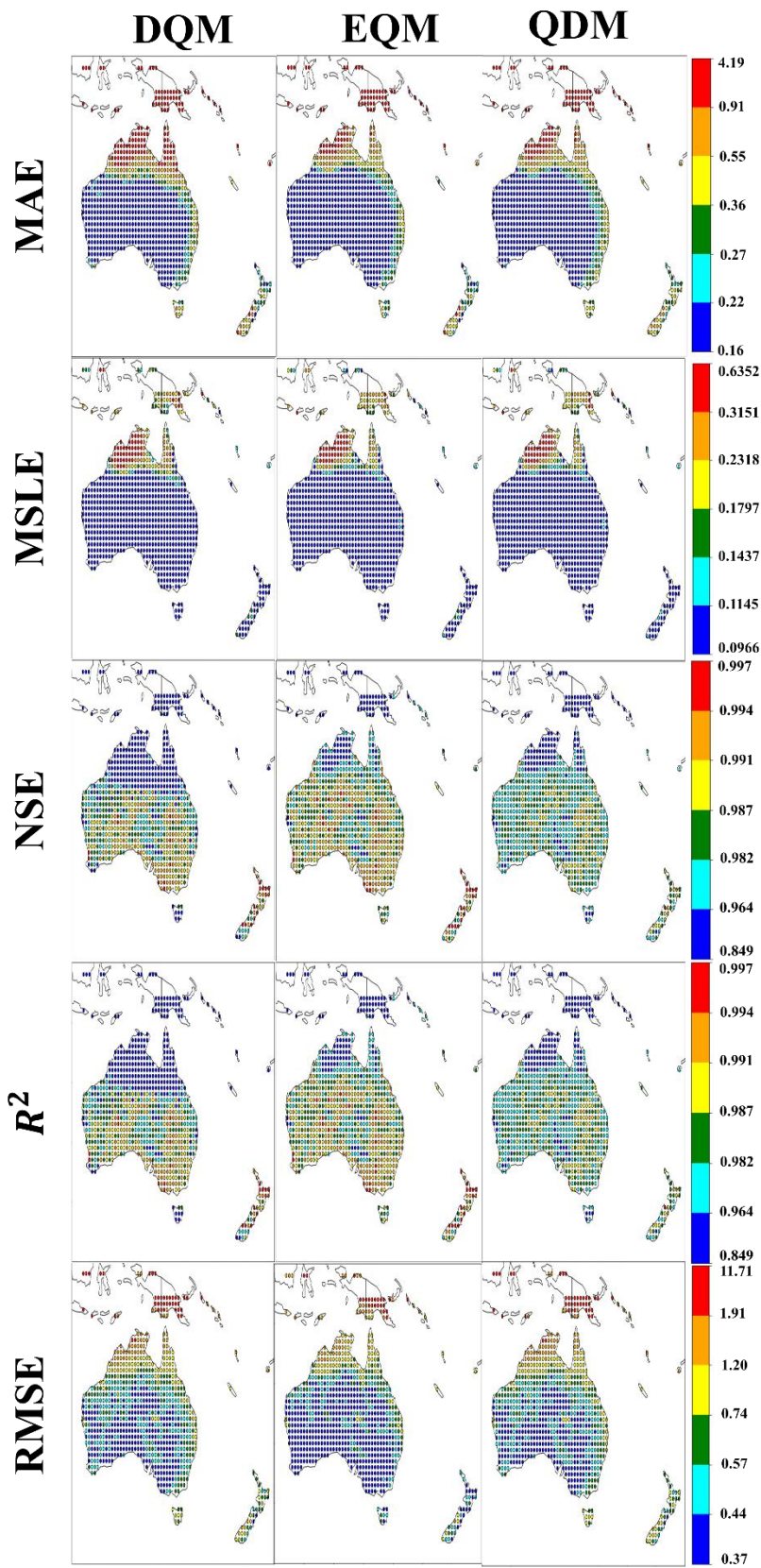


Figure 7. Performances of DQM, EQM, and QDM using evaluation metrics (MAE, MSLE, NSE, R^2 , and RMSE) for daily precipitation in Oceania.

Comment 20

L439: removed “biased”

Answer

Thank you for your comment. We have revised the sentence as follows:

Figure 9 compares the distribution differences of the daily precipitation adjusted by the bias correction methods based on the GEV distribution using the JSD.

Comment 21

L441 – 443: how does this little difference observed for the GEV method compare to the other method in terms of the differences? How does the differences observed in the other methods applied compare to the GEV method?

Answer

Thank you for your comment. Figure 9 displays the GEV distributions of the overall precipitation, with distribution differences compared to observed values using the JSD. Subsequently, Figure 10 compares the extreme precipitation values those above the 95th percentile obtained from the three QM methods.

Comment 22

L441 – 443: how does this little difference observed for the GEV method compare to the other method in terms of the differences? How does the differences observed in the other methods applied compare to the GEV method?

Answer

Thank you for your comment. We have revised the sentence as follows:

In Oceania, high weights were assigned to JSD, KGE, RMSE, and MAE, suggesting that these metrics are critical for evaluating model performance.

Comment 23

L42 – 43: This study developed.....There is no need for this sentence.

Answer

Thank you for your comment. In response, we have revised the sentence as follows:

A daily precipitation ensemble for the historical period was generated using BMA on 11 CMIP6 GCMs, and the standard deviation of daily precipitation by continent is presented as shown in Figure 14.

Comment 24

L575: What factors could contribute to the lower index observed in these regions?

Answer

These results quantify the uncertainty arising from predicting precipitation in an ensemble form using BMA on GCMs. This uncertainty is primarily attributed to differences in model structure and physical processes, model weight variance, and uncertainties in the input data. Additionally, variations in the spatial and temporal resolutions of the models and the handling of extreme events can further contribute to the overall uncertainty.

Comment 25

L615: I think “best” rather than “proper” is more suitable in this context.

Answer

Thank you for your comment. In response, we revised the sentence as follows:

QDM was selected as the best bias correction method in western North America, southern and eastern Africa, and northern Europe.

Comment 26

L653: All three methods showed strong overall performance.....This statement seems contradictory of the finding of the better performance of the EQM than the QDM and the QDM than the DQM. Authors should clarify what is meant here.

Answer

Thank you for your comment. In order to avoid confusion among readers, we revised the sentence as follows:

All three methods, as evidenced by the Taylor diagram, demonstrated overall stronger performance than the raw GCM and consistently produced good results across various regions. Nonetheless, the performance of the bias-corrected GCMs clearly differs. This highlights the need to use multiple performance metrics to fully understand the strengths and weaknesses of the three QM methods, as relying on a single analysis or macroscopic perspective can overlook important details.

Comment 27

L766: In conclusion.....I suggest authors merge this part with the conclusion section since these are some of the conclusions from the study.

Answer

Thank you for your comment. In response, we have moved the paragraph to Section 5 (Conclusion) and revised it as follows:

Generally, EQM has emerged as the preferred method due to its balanced performance, but this study emphasizes the importance of regional assessment and careful consideration of uncertainty when selecting a QM method. Furthermore, EQM is the most balanced method regarding performance and uncertainty and will likely be preferred in future climate modeling studies. However, there may be more suitable QM methods depending on the region, and a comprehensive evaluation with various weights is needed. Therefore, when establishing climate change response strategies or policy decisions, it is essential to take a multifaceted approach that considers uncertainty together rather than relying on a single indicator or performance alone. It will enable more reliable predictions and better decision-making. Future research should integrate greenhouse gas scenarios to improve the accuracy of climate predictions and provide a more comprehensive understanding of future climate risks.

Comment 28

Were there any limitations of this study. This should be discussed in a paragraph in this section as it can help guide other researchers interested in similar work in the future.

Answer

Thank you for your comment. This study has acknowledged its limitations as follows:

Future research should integrate greenhouse gas scenarios to improve the accuracy of climate predictions and provide a more comprehensive understanding of future climate risks.

Comment 29

L794: The previous bullets already talked about the conclusions. Authors can remove “In conclusion” from this line or replace it with “generally”

Answer

Thank you for your comment. In response to your comment, we have revised the paragraph as follows:

Generally, EQM has emerged as the preferred method due to its balanced performance, but this study emphasizes the importance of regional assessment and careful consideration of uncertainty when selecting a QM method. Furthermore, EQM is the most balanced method regarding performance and uncertainty and will likely be preferred in future climate modeling studies. However, there may be more suitable QM methods depending on the region, and a comprehensive evaluation with various weights is needed. Therefore, when establishing climate change response strategies or policy decisions, it is

essential to take a multifaceted approach that considers uncertainty together rather than relying on a single indicator or performance alone. It will enable more reliable predictions and better decision-making. Future research should integrate greenhouse gas scenarios to improve the accuracy of climate predictions and provide a more comprehensive understanding of future climate risks.

1 Intercomparison of bias correction methods for precipitation of 2 multiple GCMs across six continents

3 Young Hoon Song¹, Eun-Sung Chung^{1*}

4 ¹ Faculty of Civil Engineering, Seoul National University of Science and Technology, 232 G
5 ongneung-ro, Nowon-gu, Seoul 01811, Korea

6
7 * Correspondence to: Eun-Sung Chung eschung@seoultech.ac.kr

8 9 **Abstract**

10 This study, conducted across six continents, evaluated and compared the effectiveness of three
11 Quantile Mapping (QM) methods: Quantile Delta Mapping (QDM), Empirical Quantile
12 Mapping (EQM), and Detrended Quantile Mapping (DQM) for correcting daily precipitation
13 data from 11 CMIP6 General Circulation Models (GCMs). The performance of corrected
14 precipitation data was evaluated using ten evaluation metrics, and the Technique for Order of
15 Preference by Similarity to Ideal Solution (TOPSIS) was applied to calculate performance-
16 based priorities. Bayesian Model Averaging (BMA) was used to quantify model-specific and
17 ensemble prediction uncertainties. Subsequently, this study developed a comprehensive index
18 by aggregating the performance scores from TOPSIS with the uncertainty metrics from BMA.
19 **According to the results, EQM exhibited the best performance on most metrics across all**
20 **continents, with values of 0.3 (RMSE), 0.18 (MAE), 0.98 (R square), 0.87 (KGE), 0.93 (NSE),**
21 **and 0.99 (EVS), while effectively managing uncertainty with a variance of 0.0027. QDM**
22 **outperformed the other methods in specific regions and achieved the lowest model uncertainty**
23 **in South America at 0.0025. Furthermore, when greater weight was given to uncertainty, QDM**
24 **was selected more frequently than DQM by approximately 5% or more.** It suggests that daily
25 precipitation corrected by QDM is more stable than DQM. On the other hand, DQM effectively
26 reproduces dry climate but shows the highest uncertainty in certain regions, suggesting
27 potential limitations in capturing long-term climate trends. This study emphasizes that both
28 performance and uncertainty should be considered when choosing a bias correction method to
29 increase the reliability of climate predictions.

31 **Keywords**

32 CMIP6 GCM, Bias correction, Uncertainty, TOPSIS, Comprehensive index

33

34 1. Introduction

35 The Coupled Model Intercomparison Project (CMIP) General Circulation Models
36 (GCMs) have provided critical scientific evidence to explore climate change (IPCC, 2021;
37 IPCC, 2022). Nevertheless, GCMs exhibit significant biases compared to observational data
38 for reasons such as incomplete model parameterization and inadequate understanding of key
39 physical processes (Evin et al., 2024; Zhang et al., 2024; Nair et al., 2023). These deficiencies
40 with GCM have introduced various uncertainties in climate projections, making ensuring
41 sufficient reliability in climate change impact assessments difficult. In this context, many
42 studies have proposed various bias correction methods to reduce the discrepancies between
43 observational data and GCM simulations, thereby providing more stable results than raw GCM-
44 based assessments (Cannon et al., 2015; Themeßl et al., 2012; Piani et al., 2010). Despite these
45 advancements, the suggested bias correction methods differ in their physical approaches,
46 resulting in discrepancies in the climate variables adjusted for historical periods. Furthermore,
47 the distribution of precipitation across continents and specific locations causes variations in the
48 correction outcomes depending on the method used, which makes it challenging to reflect
49 extreme climate events in future projections and adds another layer of confusion to climate
50 change research (Song et al., 2022b; Maraëun, 2013; Ehret et al., 2012; Enayati et al., 2021).
51 Thus, exploring multiple aspects to make reasonable selections when applying bias correction
52 methods specific to each continent and region is necessary.

53 Many studies have developed appropriate bias correction methods based on various
54 theories, which have reduced the difference between raw GCM simulations and observed
55 precipitation (Abdelmoaty and Papalexiou, 2023; Shanmugam et al., 2024; Rahimi et al., 2021).
56 The Quantile Mapping (QM) series has been widely adopted among bias correction methods
57 due to its conceptual simplicity, ease of application, and adaptability to various methodologies.
58 However, although standard QM methods have high performance in correcting stationary
59 precipitation, they are less efficient in non-stationary data, such as extreme precipitation events
60 (Song et al., 2022b). To address these limitations, recent studies proposed an improved QM
61 approach to reflect future non-stationary precipitation across all quantiles of historical
62 precipitation (Rajulapati and Papalexiou, 2023; Cannon et al., 2015; Cannon, 2018; Song et al.,
63 2022b). In recent years, climate studies using GCMs have adopted several improved QM
64 methods that offer higher performance than previous methods to correct historical precipitation
65 and project it accurately into the future. For example, Song et al. (2022b) performed bias

66 correction on daily historical precipitation over South Korea using distribution transformation
67 methods they developed and found that the best QM method varied depending on the station.
68 Additionally, previous studies have reported that QM performance varied by grid and station
69 (Ishizaki et al., 2022; Chua et al., 2022). **Furthermore, they compared the extreme precipitation
70 of GCMs using the GEV distribution, which allows for more effective estimation of extreme
71 precipitation, and demonstrated that the performance in estimating extreme precipitation varies
72 according to different bias correction methods.** From this perspective, these improved QMs
73 may only guarantee uniform results across some grids and regions. Therefore, to analyze
74 positive changes in future climate impact assessments, selecting appropriate bias correction
75 methods based on a robust framework is essential.

76 Multi-criteria decision analysis (MCDA) is efficient for prioritization because it can
77 aggregate diverse information from various alternatives. MCDA has been extensively used
78 across different fields to select suitable alternatives, with numerous studies confirming its
79 stability in priority selection (Chae et al., 2022; Chung and Kim, 2014; Song et al., 2024a).
80 Moreover, MCDA has been employed in future climate change studies to provide reasonable
81 solutions to emerging problems, including the selection of bias correction methods for specific
82 regions and countries (Homsy et al., 2019; Saranya and Vinish, 2021). **Technique for Order
83 Preference by Similarity to Ideal Solution (TOPSIS) is effectively utilized in our study's
84 MCDA framework by integrating multiple evaluation metrics and calculating the distance
85 between each alternative and the ideal solution, thereby enabling clear and intuitive
86 prioritization decisions.** However, MCDA's effectiveness is sensitive to the source and quality
87 of alternatives, making accurate ranking challenging when information is lacking or overly
88 focused on specific criteria (Song and Chung, 2016). Small-scale regional and observation-
89 based studies have conducted GCM performance evaluations, but global and continental-scale
90 evaluations are rare due to the substantial time and cost required.

91 GCM simulation includes uncertainties from various sources, such as model structure,
92 initial condition, boundary condition, and parameters (Pathak et al., 2023; Cox and Stephenson,
93 2007; Yip et al., 2011; Woldemeskel et al., 2014). The selection of bias correction methods
94 contributes significantly to uncertainty in climate change research using GCMs. Jobst et al.
95 (2018) argued that GHG emission scenarios, bias correction methods, and GCMs are primary
96 sources of uncertainty in climate change assessments across various fields. The extensive
97 uncertainties in GCMs complicate the efficient establishment of adaptation and mitigation

98 policies. This issue has increased awareness of the uncertainties inherent in historical
99 simulations. Consequently, many studies have focused on estimating uncertainties using
100 diverse methods to quantify these uncertainties (Giorgi and Mearns, 2002; Song et al., 2022a;
101 Song et al., 2023). Although it is impossible to drastically reduce the uncertainty of GCM
102 outputs due to the unpredictable nature of climate phenomena, uncertainties in GCM
103 simulations can be reduced using ensemble principles, such as multi-model ensemble
104 development using a rational approach (Song et al., 2024). **However, accurately identifying
105 biases in precipitation simulation remains challenging due to the lack of comprehensive
106 equations reflecting Earth's physical processes.** In this context, climate change studies have
107 aimed to quantify the uncertainty of historical climate variables in GCMs, offering insights into
108 the variability of GCM simulations (Pathak et al., 2023). Bias-corrected precipitation of GCMs
109 using QM has shown high performance in the historical period, which is expected to result in
110 better future predictions. However, the physical concepts of various QMs may lead to more
111 significant uncertainty in the future (Lafferty et al., 2023). Therefore, efforts should be made
112 to consider and reduce uncertainty in the GCM selection process. It will ensure the reliability
113 of predictions by selecting an appropriate bias-correcting method. **Furthermore, Bayesian
114 Model Averaging (BMA) plays a crucial role in quantifying the predictive uncertainty of
115 multiple climate models and enhancing the reliability of the final predictions, which is why it
116 has been employed as an indispensable tool in our integrated evaluation.**

117 **In light of the challenges outlined above, including discrepancies among bias
118 correction methods, regional variability in precipitation distributions, and significant
119 uncertainties in GCM outputs, there is a clear need for an integrated framework that evaluates
120 the performance of various QM methods and quantifies their associated uncertainties.** This
121 study aims to compare the performance of three bias correction methods using daily historical
122 precipitation data (1980-2014) from CMIP6 GCMs across six continents (South America: SA;
123 North America: NA; Africa: AF; Europe: EU; Asia: AS; and Oceania: OA). Ten evaluation
124 metrics were used to assess the performance of daily precipitation corrected by the three QM
125 methods for each continent. Subsequently, the Technique for Order of Preference by Similarity
126 to Ideal Solution (TOPSIS) of MCDA was applied to select an appropriate bias correction
127 method for each continent. Additionally, the uncertainty in daily precipitation for historical
128 periods was quantified using BMA. By integrating performance scores from TOPSIS and
129 uncertainty metrics from BMA, this study developed a Comprehensive Index (CI), which was

130 then used to select the best bias correction method for each continent. This comprehensive
 131 approach ensures a balanced consideration of both performance and uncertainty, enhancing
 132 understanding of the bias correction process based on the distribution of daily precipitation
 133 across continents.

134

135 **2. Datasets and methods**

136 **2.1 General Circulation Model**

137 This study used 11 CMIP6 GCM to perform bias correction for daily precipitation in the
 138 historical period. The variant label for the GCMs used in this study was r1i1p1f1. Table 1
 139 presents basic information, including model names, resolution. The model resolution of 11
 140 CMIP6 GCMs was equally re-gridded to $1^\circ \times 1^\circ$ using linear interpolation. Furthermore, this
 141 study's ensemble member of CMIP6 GCMs was the first member of realizations (r1).

142

143 **Table 1. Information of CMIP6 GCMs in this study**

Institution	Models	Resolution
Commonwealth scientific and industrial research organization/ Australia	ACCESS-CM2	$1.2^\circ \times 1.8^\circ$
	ACCESS-ESM1-5	$1.2^\circ \times 1.8^\circ$
Beijing Climate Center/China	BCC-CSM2-MR	$1.1^\circ \times 1.1^\circ$
Canadian Centre for Climate Modeling and Analysis/ Canada	CanESM5	$2.8^\circ \times 2.8^\circ$
National Center for Atmospheric Research	CESM2-WACCM	$0.9^\circ \times 1.3^\circ$
Euro-Mediterranean Center on Climate Change coupled climate model/ Italy	CMCC-CM2-SR5	$\sim 0.9^\circ$
	CMCC-ESM2	$0.9^\circ \times 1.25^\circ$
EC-Earth Climate Model Consortium/ EC-EARTH consortium	EC-Earth3-Veg-LR	$1.0^\circ \times 1.0^\circ$
National Oceanic and Atmospheric Administration/ United States	GFDL-ESM4	$1.4^\circ \times 1.4^\circ$
Institute for Numerical Mathematics/ Russia	INM-CM4-8	$\sim 0.9^\circ$
Institute Pierre Simon Laplace/ France	IPSL-CM6A-LR	$1.1^\circ \times 1.1^\circ$

144

145 **2.2 Reference data**

146 This study utilized re-gridded precipitation data derived from ERA5 reanalysis products
 147 provided by the European Centre for Medium-Range Weather Forecasts (ECMWF). The
 148 original ERA5 precipitation data, available at a $0.25^\circ \times 0.25^\circ$ spatial resolution, was re-gridded
 149 to a $1.0^\circ \times 1.0^\circ$ resolution using the Python library xESMF. The data units were converted from
 150 meters per day (m/day) to millimeters per day (mm/day) for consistency with other datasets.
 151 The dataset is part of the FROGS (Frequent Rainfall Observations on Grids) database, which

152 integrates various precipitation products, including satellite-based, gauge-based, and reanalysis
 153 data (Roca et al., 2019). The re-gridded dataset was selected for its spatial compatibility with
 154 the study's objectives, facilitating the evaluation of General Circulation Model (GCM)
 155 simulations in replicating observed precipitation patterns. The FROGS database provides a
 156 robust framework for intercomparison and assessment of precipitation products across different
 157 sources. FROGS database has been widely used in various studies to ensure the reliability of
 158 climate model evaluation and climate change assessment (Wood et al., 2021; Roca and Fiolleau,
 159 2020; Petrova et al., 2024).

160

161 **2.3 Quantile mapping**

162 This study employed three (Quantile delta mapping, QDM; Detrended quantile mapping, DQM;
 163 Empirical quantile mapping, EQM) QM methods to correct the simulation of CMIP6 GCMs,
 164 and these methods are commonly used in climate change research based on the climate models
 165 (Switanek et al., 2017). This study divided the data into a training period (1980-1996) and a
 166 validation period (1997-2014) to correct the historical period's data. This approach minimizes
 167 the influence of uncertainties associated with future projections, allowing the study to focus on
 168 evaluating the intrinsic performance differences of the QM methods. The frequency-adaptation
 169 technique, as described by Themeßl et al. (2012), was applied to address potential biases and
 170 improve the accuracy of the corrections. The corrected precipitation using the QM used a
 171 cumulative distribution function, as shown in Equation 1, to reduce the difference from the
 172 reference data.

$$173 \hat{x}_{m,p}(t) = F_{o,h}^{-1}\{F_{m,h}[x_{m,p}(t)]\} \quad (1)$$

174 where, $\hat{x}_{m,p}(t)$ presents the bias-corrected results. $F_{o,h}$ represents the cumulative distribution
 175 function (CDF) of the observed data, and $F_{m,h}$ presents the CDF of the model data. The
 176 subscripts o and m denote observed and model data, respectively, and the subscript h denotes
 177 the historical period.

178 QDM, developed by Cannon et al. (2015), preserves the relative changes ratio of modeled
 179 precipitation quantiles. In this context, QDM consists of bias correction terms derived from
 180 observed data and relative change terms obtained from the model. The computation process of
 181 QDM is carried out as described in Equation (2) to (4).

$$182 \hat{x}_{m,p}(t) = \hat{x}_{o:m,h;p}(t) \cdot \Delta_m(t) \quad (2)$$

$$183 \hat{x}_{o:m,h;p}(t) = F_{o,h}^{-1}[F_{m,p}^{(t)}\{x_{m,p}(t)\}] \quad (3)$$

$$184 \quad \Delta_m(t) = \frac{x_{m,p}(t)}{F_{m,h}^{-1}[F_{m,p}^{(t)}\{x_{m,p}(t)\}]} \quad (4)$$

185 where, $\hat{x}_{o:m,h:p}(t)$ presents the bias corrected daily precipitation for the historical period, and
 186 $\Delta_m(t)$ the relative change in the model simulation between the reference period and the target
 187 period. In addition, the target period is calculated by multiplying the relative change ($\Delta_m(t)$)
 188 at time (t) multiplied by the bias-corrected precipitation in the reference period. $\Delta_m(t)$ is
 189 defined as $\widehat{x_{m,p}}(t)$ divided by $F_{o,h}^{-1}[F_{m,p}^{(t)}\{x_{m,p}(t)\}]$. $\Delta_m(t)$ preserving the relative change
 190 between the reference and target periods. DQM, while more limited compared to QDM,
 191 integrates additional information regarding the projection of future precipitation. Furthermore,
 192 climate change signals estimated from DQM tend to be consistent with signals from baseline
 193 climate models. The computational process of DQM is performed as shown in Equation (5).

$$194 \quad \hat{x}_{m,p} = F_{o,h}^{-1} \left\{ F_{m,h} \left[\frac{\bar{x}_{m,h} x_{m,h}(t)}{\bar{x}_{m,p}(t)} \right] \right\} \frac{\bar{x}_{m,p}(t)}{\bar{x}_{m,h}} \quad (5)$$

195 where, $\bar{x}_{m,h}$ and $\bar{x}_{m,p}$ represent the long-term modeled averages for the historical reference
 196 period and the target period, respectively.

197 EQM is a method that corrects the quantiles of the empirical cumulative distribution function
 198 from a GCM simulation based on a reference precipitation distribution using a corrected
 199 transfer function (Dequé, 2007). The calculation process of EQM can be represented as follows
 200 in Equation (6).

$$201 \quad \hat{x}_{m,p}(t) = F_{o,h}^{-1}(F_{m,h}(x_{m,p}(t))) \quad (6)$$

202 All these QMs can be applied to historical data correction in this approach. The bias correction
 203 is performed based on the relative changes between a reference period and a target period in
 204 the past, ensuring that the relative changes between these periods are preserved in the corrected
 205 data (Ansari et al., 2023; Tanimu et al., 2024; Cannon et al., 2015).

206

207 **2.4 Evaluation metrics**

208 This study used ten evaluation metrics to assess the output performance of three quantile
 209 mapping methods against the reference data for the validation period (1997-2014). **Ten**
 210 **evaluation metrics used in this study are as follows: Root Mean Square Error (RMSE), Mean**
 211 **Absolute Error (MAE), Coefficient of Determination (R^2), Percent bias (Pbias), Nash-Sutcliffe**
 212 **Efficiency (NSE), Kling-Gupta efficiency (KGE), Median Absolute Error (MdAE), Mean**
 213 **Squared Logarithmic Error (MSLE), Explained Variance Score (EVS), and Jenson-Shannon**
 214 **divergence (JS-D).** The equations of seven evaluation metrics are presented in Table 2.

Metrics	Equations	Factors	References
RMSE	$= \sqrt{\frac{1}{n} \sum_{i=1}^n (X_i^{sim} - X_i^{ref})^2}$		
MAE	$= \sum_{i=1}^n X_i^{sim} - X_i^{ref} $		
R^2	$= 1 - \frac{\sum_{i=1}^n (X_i^{sim} - X_i^{ref})^2}{(X_i^{ref} - \bar{X}_i^{ref})^2}$		Galton, 1886
Pbias	$= \frac{\sum_{i=1}^n (X_i^{ref} - X_i^{sim})}{\sum_{i=1}^n X_i^{ref}} \times 100$	X_i^{ref} reference data X_i^{sim} Bias	
NSE	$= 1 - \frac{\sum_{i=1}^n (X_i^{sim} - X_i^{ref})^2}{\sum_{i=1}^n (X_i^{ref} - \bar{X}_i^{ref})^2}$	corrected GCM	Nash and Sutcliffe, 1970
MdAE	$= \text{median}(X_i^{sim} - X_i^{ref})$		
MSLE	$= \frac{1}{n} \sum_{i=1}^n (\log(1 + X_i^{sim}) - \log(1 + X_i^{ref}))^2$		
EVS	$= 1 - \frac{\text{Var}(X^{sim} - X^{ref})}{\text{Var}(X^{ref})}$		
KGE	$= 1 - \sqrt{(r - 1)^2 + (\alpha - 1)^2 + (\beta - 1)^2}$	r Pearson product- moment correlation α Variability error β : Bias term	Gupta et al. 2009

JS-D	$= \frac{1}{2}D_{KL} \left(P \parallel \frac{P+Q}{2} \right) + \frac{1}{2}D_{KL} \left(Q \parallel \frac{P+Q}{2} \right)$	$P(x)$: Probability density distribution of reference data $Q(x)$: Probability density distribution of GCM D_{KL} : KL-D	Lin, 1991
------	---	--	-----------

217

218 Ten evaluation metrics selected in this study assess GCM performance from various
 219 perspectives, including error (RMSE, MAE, MdAE, and MSLE), deviation (Pbias), accuracy (R^2 , NSE), variability (EVS), correlation and overall performance (KGE), and distributional
 220 differences (JSD). These metrics complement each other by offering a comprehensive
 221 evaluation framework. For instance, while NSE evaluates the overall fit of the simulated data
 222 to observations, KGE provides a holistic view by integrating correlation, variability, and bias
 223 into a single efficiency score, and JS-D captures the difference between the distributions of the
 224 reference data and the bias-corrected GCM output.
 225

226

227 2.5 Generalized extreme value

228 This study used generalized extreme value (GEV) to compare the extreme precipitation
 229 calculated by the bias-corrected GCM at each grid of six continents over the historical period.
 230 The historical precipitation was compared with the distribution of reference data and bias-
 231 corrected GCM above the 95th quantile of the Probability Density Function (PDF) of the GEV
 232 distribution (Hosking et al. 1985). In addition, this study compared the distribution differences
 233 between the reference data based on the GEV distribution and the corrected GCM using JSD.
 234 GEV distribution is commonly used to confirm extreme values in climate variables. The PDF
 235 of the GEV distribution is shown in Equation 7, and the parameters of the GEV distribution
 236 were estimated using L-moment (Hosking, 1990).

$$237 \quad g(x) = \frac{1}{\alpha} \left[1 - k \frac{x-\epsilon}{\alpha} \right]^{\frac{1}{k}-1} \exp \left\{ - \left[1 - k \frac{x-\epsilon}{\alpha} \right]^{\frac{1}{k}} \right\} \quad (7)$$

238 where, k , α , and ϵ represents a shape, scale, and location of the GEV distribution, respectively.

239

240 2.6 Bayesian model averaging (BMA)

241 The BMA is a statistical technique that combines multiple models to provide predictions that
 242 account for model uncertainty (Hoeting et al., 1999). BMA is used to integrate predictions from
 243 GCMs to improve the robustness and reliability of the resulting assemblies. The posterior
 244 probability of each model is calculated based on Bayes' theorem as shown in Equation 8.

$$245 \quad P(M_k | D) = \frac{P(D|M_k)P(M_k)}{\sum_{j=1}^K P(D|M_j)P(M_j)} \quad (8)$$

246 where, $P(M_k)$ is the prior probability of model M_k , and $P(D | M_k)$ is the likelihood of the data
 247 D given model M_k , $P(M_k | D)$ is the posterior probability of model M_k . In addition, the BMA
 248 prediction \hat{Q}_{BMA} is the weighted average of the predictions from each model as shown in
 249 Equation 9.

$$250 \quad \hat{Q}_{BMA} = \sum_{k=1}^K P(M_k | D) \hat{Q}_k \quad (9)$$

251 where, \hat{Q}_k is the prediction from model M_k . In this study, BMA was used to quantify the model
 252 uncertainty and ensemble prediction uncertainty for daily precipitation corrected by three QM
 253 methods (QDM, EQM, and DQM) applied to 11 CMIP6 GCMs, as shown in Equations 10 and
 254 11.

$$255 \quad \alpha_w^2 = \frac{1}{K} \sum_{k=1}^K (w_k - \bar{w})^2 \quad (10)$$

256 where, K is the number of models, $w_k = P(M_k | D)$ is the weight of model M_k , \bar{w} is the mean
 257 of the weights, given by $\bar{w} = \frac{1}{K} \sum_{k=1}^K w_k$. A higher variance in model weights indicates more
 258 significant prediction differences, implying greater model uncertainty.

$$259 \quad \sigma_{BMA} = \sqrt{\frac{1}{K} \sum_{k=1}^K (\hat{Q}_k - \hat{Q}_{BMA})^2} \quad (11)$$

260 σ_{BMA} is standard deviation of the BMA ensemble predictions, \hat{Q}_k is the prediction from each
 261 model M_k , \hat{Q}_{BMA} is the weighted average prediction from BMA. This standard deviation
 262 represents the variability among the ensemble predictions and serves as an indicator of
 263 uncertainty. A lower standard deviation implies higher consistency among predictions,
 264 indicating lower uncertainty, while a higher standard deviation suggests greater variability and
 265 higher uncertainty.

266

267 **2.7 TOPSIS**

268 This study used TOPSIS to calculate a rational priority among three QM methods based on the
 269 outcomes derived from evaluation metrics. Furthermore, the closeness coefficient calculated
 270 using TOPSIS was used as the performance metric for the CI. Proposed by Hwang and Yoon

271 (1981), TOPSIS is a multi-criteria decision-making technique frequently used in water
 272 resources and climate change research to select alternatives (Song et al., 2024). As described
 273 in Equation 12 and 13, the proximity of the three QM methods is calculated based on the
 274 Positive Ideal Solution (PIS) and the Negative Ideal Solution (NIS).

$$275 \quad D_i^+ = \sqrt{\sum_{j=1}^n w_j (f_j^+ - f_{i,j})^2} \quad (12)$$

$$276 \quad D_i^- = \sqrt{\sum_{j=1}^n w_j (f_j^- - f_{i,j})^2} \quad (13)$$

277 where, D_i^+ is the Euclidean distance of each criterion from the PIS, summing the whole criteria
 278 for an alternative f_j^+ , j presents the normalized value for the alternative f_j^+ . w_j presents weight
 279 assigned to the criterion j . D_i^- is the distance between the alternative f_j^- and the NIS. The
 280 relative closeness is calculated as shown in Equation 14. The optimal value is closer to 1 and
 281 represents a reasonable alternative.

$$282 \quad C_i = \frac{D_i^-}{(D_i^- + D_i^+)} \quad (14)$$

283 **This study used entropy theory to calculate the weights for each criterion. Entropy weighting**
 284 **ensures sufficient objectivity by calculating weights based on the variability and distribution**
 285 **of data. This approach minimizes subjectivity, preventing biases in the weighting process.**

286

287 **2.8 Comprehensive index (CI)**

288 This study proposed a CI to select the best QM method by combining performance scores and
 289 model uncertainty indicators. The CI integrates the performance scores (closeness coefficient)
 290 derived from the TOPSIS method with the uncertainty quantified using BMA. This approach
 291 allows for a balanced evaluation that considers both the effectiveness of the QM methods and
 292 the associated uncertainties. Uncertainty was quantified in two ways. Model-specific weight
 293 variance was calculated using the variance of the model weights assigned by BMA,
 294 representing the uncertainty in selecting the appropriate QM. The standard deviation of BMA
 295 ensemble prediction was calculated to capture the spread and, thus, the uncertainty of the
 296 ensemble forecasts. Both the indicators were normalized using a min-max scaler to ensure
 297 comparability. **The CI is calculated individually for every grid and can reflect climate**
 298 **characteristics. Framework provides flexibility in determining the weighting of uncertainty or**
 299 **performance depending on the study objectives. Additionally, the methodology offers**
 300 **flexibility in selecting performance and uncertainty metrics. Alternative MCDA methods**

301 beyond TOPSIS can be utilized for performance indicators, or indices that effectively represent
302 the model's performance can be employed to calculate the CI. Similarly, for uncertainty
303 indicators, approaches such as variance, standard deviation, or other uncertainty quantification
304 techniques can be applied to enhance the robustness of the framework further. Finally, the
305 calculation process of the CI is performed as shown in Equations 15 and 16.

$$306 \quad UI = \frac{V_w + \sigma_e}{2} \quad (15)$$

$$307 \quad CI = \alpha \times C_i - \beta \times UI \quad (16)$$

308 where, UI represents the uncertainty indicator. V_w and σ_e represent the normalized weight
309 variance and the normalized ensemble standard deviation, respectively, calculated using BMA.
310 C_i represents the closeness coefficient calculated from TOPSIS. α represents the weight given
311 to the performance score, β represents the weight given to the uncertainty indicator.
312 Furthermore, by adjusting the weights α and β , the study evaluated the QM methods under
313 different scenarios. Equal weight ($\alpha = 0.5$, $\beta = 0.5$) balances performance and uncertainty
314 equally, and the emphasized performance weight ($\alpha = 0.7$, $\beta = 0.3$) prioritize performance over
315 uncertainty. The emphasized uncertainty weight ($\alpha = 0.3$, $\beta = 0.7$) prioritize uncertainty over
316 performance. The results from the CI provide a holistic evaluation of the QM methods,
317 considering both their effectiveness in bias correction and the reliability of their predictions.

318

319 **3. Result**

320 **3.1 Assessment of bias correction reproducibility across continents**

321 **3.1.1 Comparison of bias correction effects**

322 A Taylor diagram was used to compare the bias-corrected and raw GCM precipitation with the
323 observed data, and Figure 1 presents the results of applying the three QM methods to 11 CMIP6
324 GCMs. In general, the precipitation corrected by DQM showed a larger difference from the
325 reference data than other methods. In contrast, EQM performed better than DQM, and many
326 models showed results close to the reference data. The precipitation corrected by QDM also
327 showed good performance in most continents but slightly lower than EQM. Nevertheless,
328 QDM showed clearly better results than DQM.

329 Regarding correlation coefficients, precipitation corrected by DQM showed relatively high
330 values between 0.8 and 0.9 but lower than EQM and QDM. The precipitation corrected by
331 EQM showed high agreement with the reference data, recording correlation coefficients above

332 0.9 in most continents. QDM generally showed similar correlation coefficients to EQM but
333 slightly lower values than EQM in North America and Asia.

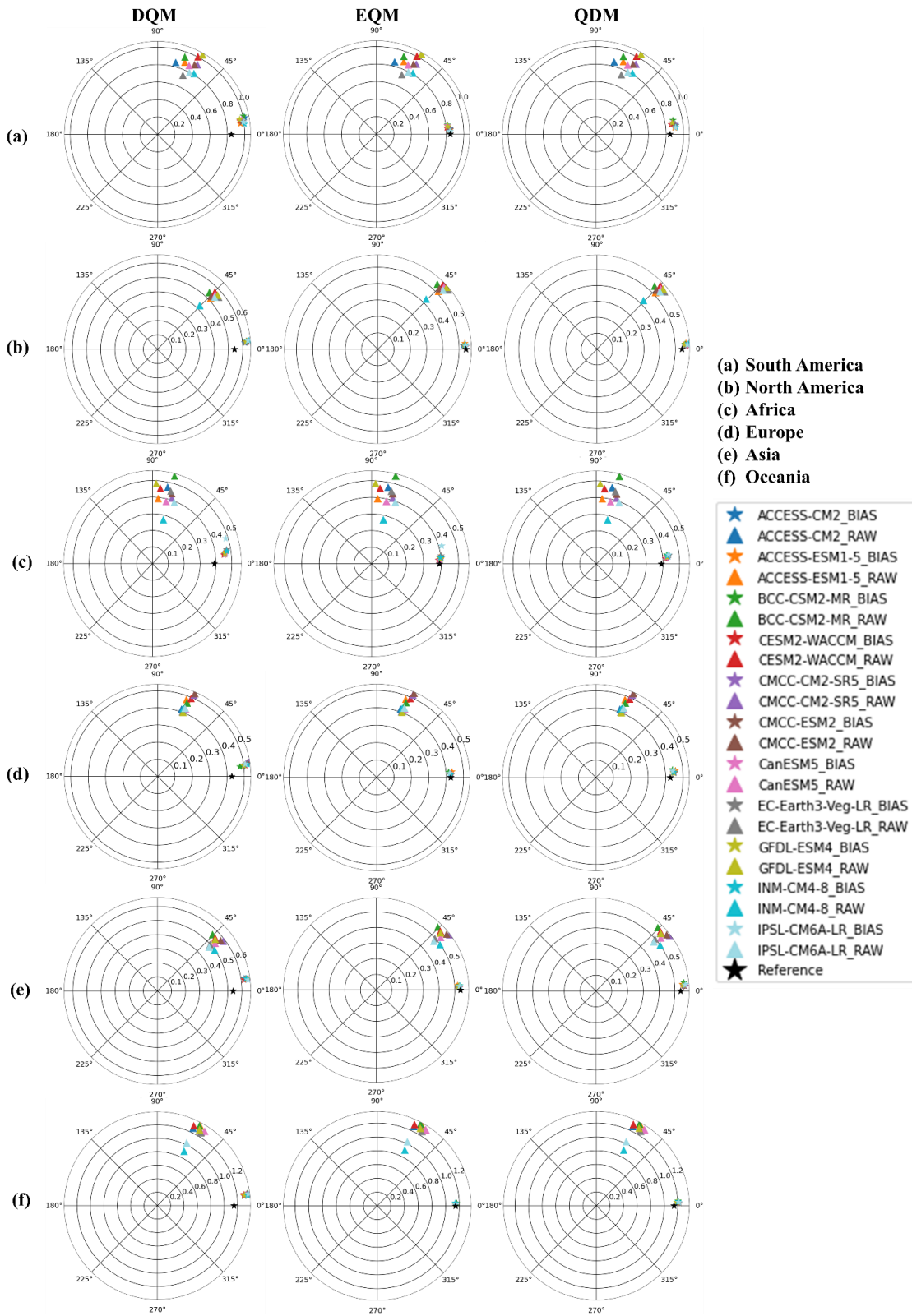
334 For RMSE, precipitation corrected by DQM was higher than EQM and QDM, indicating that
335 the corrected precipitation differed more from the reference data. On the other hand, EQM had
336 the lowest RMSE and showed superior performance compared to other methods. QDM had
337 slightly higher RMSE than EQM but still outperformed DQM.

338 In terms of standard deviation, precipitation corrected by DQM was higher or lower than the
339 reference data in most continents. On the other hand, precipitation corrected by EQM was
340 similar to the reference data and almost identical to the reference data in Africa and Asia. QDM
341 was similar to the reference data in some continents but showed slight differences from EQM.

342 These results imply that the precipitation corrected by the three methods outperforms the raw
343 simulation, which confirms that the GCM's daily precipitation is reliably corrected in the
344 historical period.

345

Taylor diagram



346

347 Figure 1. Comparison of raw and corrected daily precipitation on six continents using Taylor

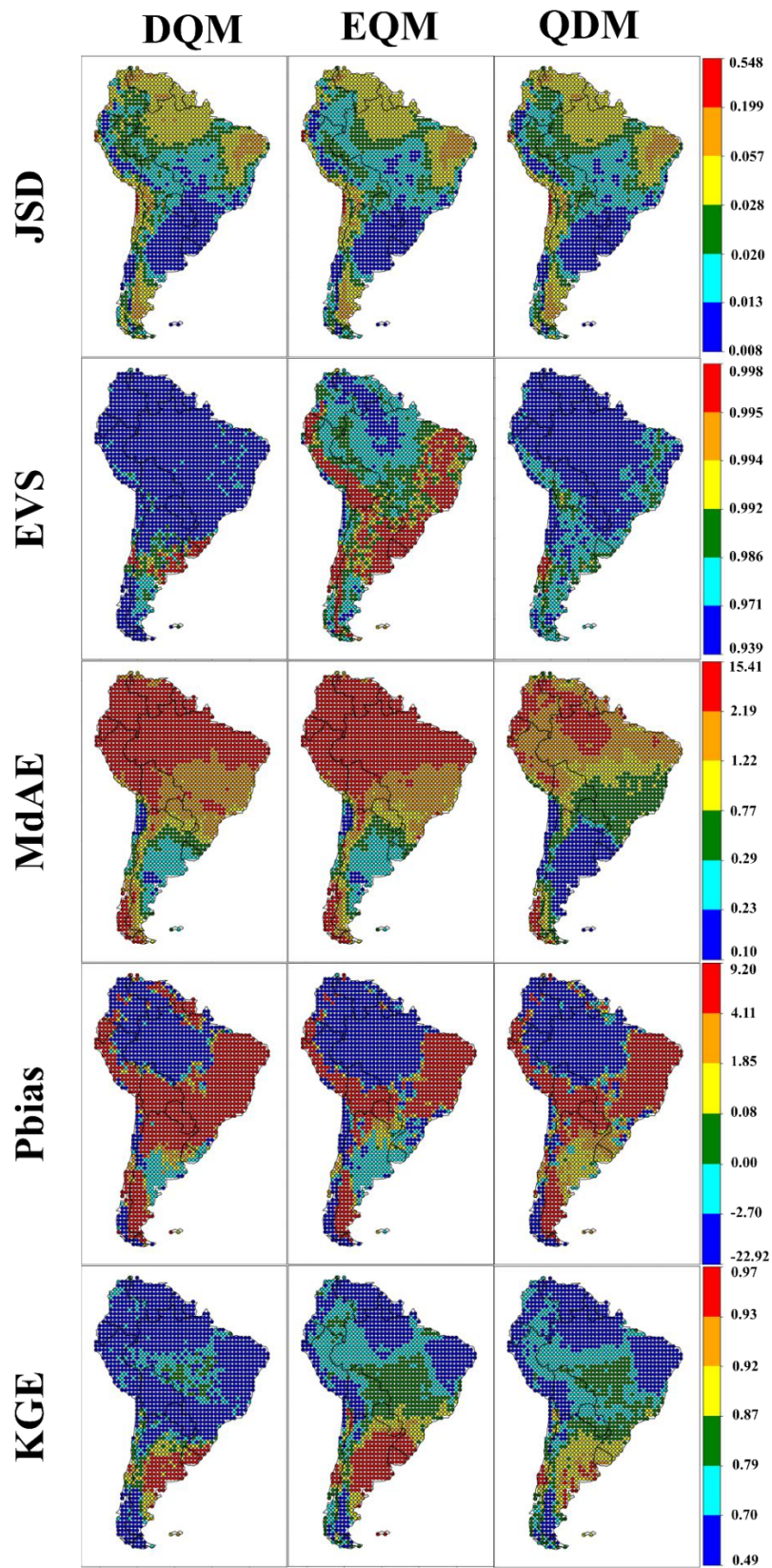
348 diagrams

349 **3.1.2 Spatial distribution of bias correction performance**

350 The spatial patterns of the evaluation metrics computed from the bias-corrected daily
351 precipitation data of GCMs in South America are presented as shown in Figures 2 and S1.

352 Overall, the precipitation corrected by EQM demonstrated lower JSD values, as well as higher
353 EVS and KGE values, compared to other methods. The precipitation corrected by EQM
354 showed higher EVS in certain regions but slightly lower performance in MDAE and Pbias
355 across some grids. DQM exhibited performance similar to EQM and QDM in most evaluation
356 indices but was relatively lower in most evaluation metrics. The precipitation corrected by the
357 three methods was underestimated compared to the reference data in northern South America,
358 while it was overestimated in eastern South America. In addition, precipitation corrected by
359 the DQM method tended to be overestimated more than the other methods, while the EQM
360 method showed the opposite result. Furthermore, the daily precipitation corrected by EQM
361 showed the lowest overall error and high performance in both NSE and R^2 . QDM and DQM
362 also performed well but exhibited slightly larger errors in some regions than EQM.

363



364

365 Figure 2. Performance comparison of DQM, EQM, and QDM using evaluation metrics (JSD,

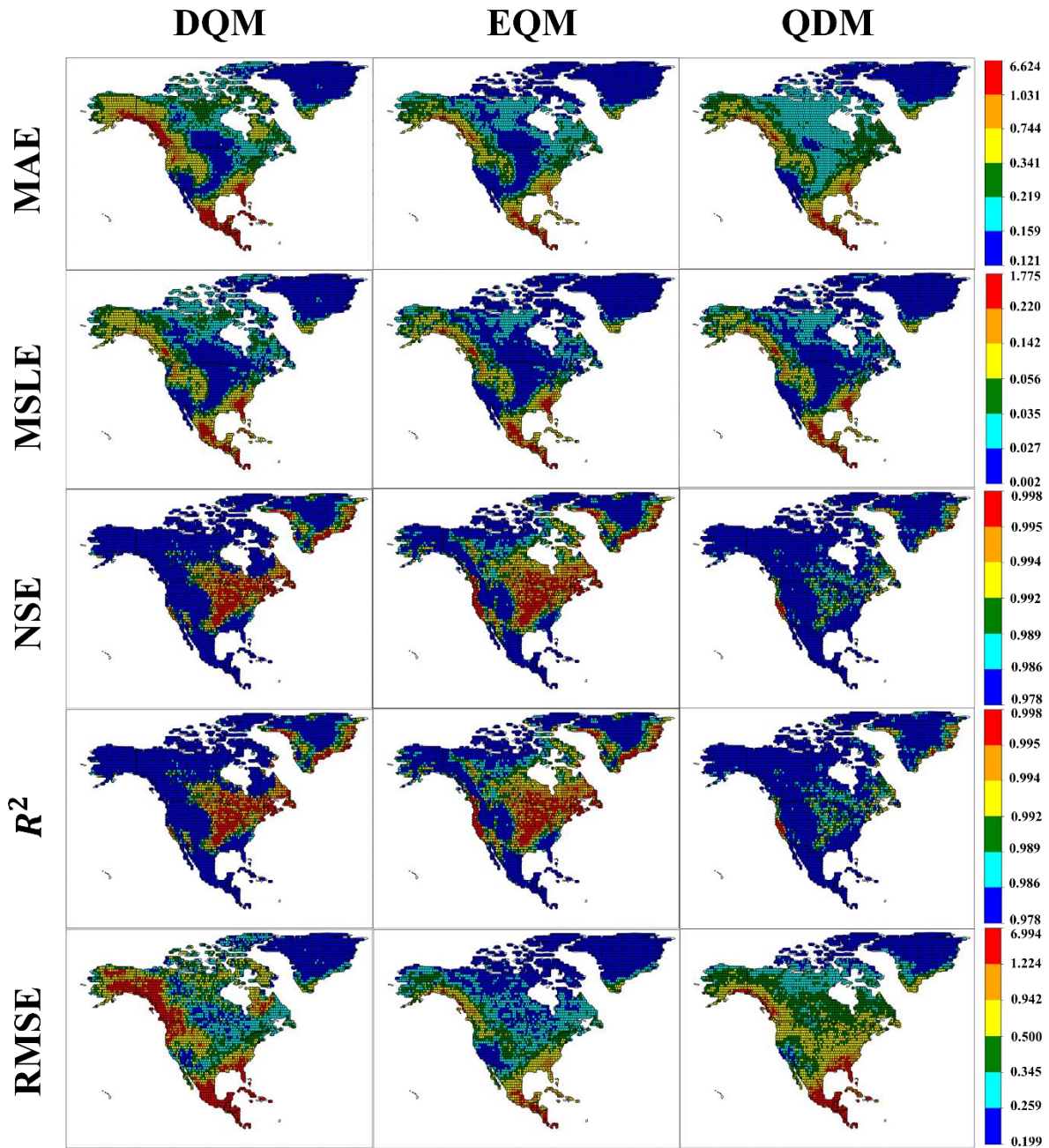
366 EVS, MdAE, Pbias, and KGE) for daily precipitation in South America.

367 **Figures 3 and S2 present the spatial patterns of these evaluation metrics, calculated for daily**
368 **precipitation from the bias corrected GCMs in North America.** Regarding error metrics (MAE,
369 MSLE, RMSE, and MdAE), precipitation corrected using DQM showed relatively lower
370 performance across North America, with substantial errors in the southern region. In contrast,
371 precipitation corrected using EQM demonstrated superior performance across the continent
372 compared to other methods. QDM exhibited similar error performance to EQM but slightly
373 higher errors in the southern region.

374 For correlation metrics (NSE and R^2), DQM-corrected precipitation had lower performance
375 than other methods, although some grid cells in the central and eastern regions showed high
376 performance, with values exceeding 0.995. The precipitation corrected using EQM showed the
377 highest performance, especially in the central and eastern regions, where most grid points
378 showed correlation coefficients above 0.995. QDM, while achieving correlation metrics above
379 0.978 for most grid points, had slightly lower performance than the other methods.

380 Regarding Pbias, all three methods tended to overestimate precipitation relative to the reference
381 data across most grid points in North America, while corrected precipitation in Greenland was
382 underestimated. For JSD, EVS, and KGE metrics, EQM-corrected precipitation showed the
383 highest performance, with DQM and QDM performing lower than EQM.

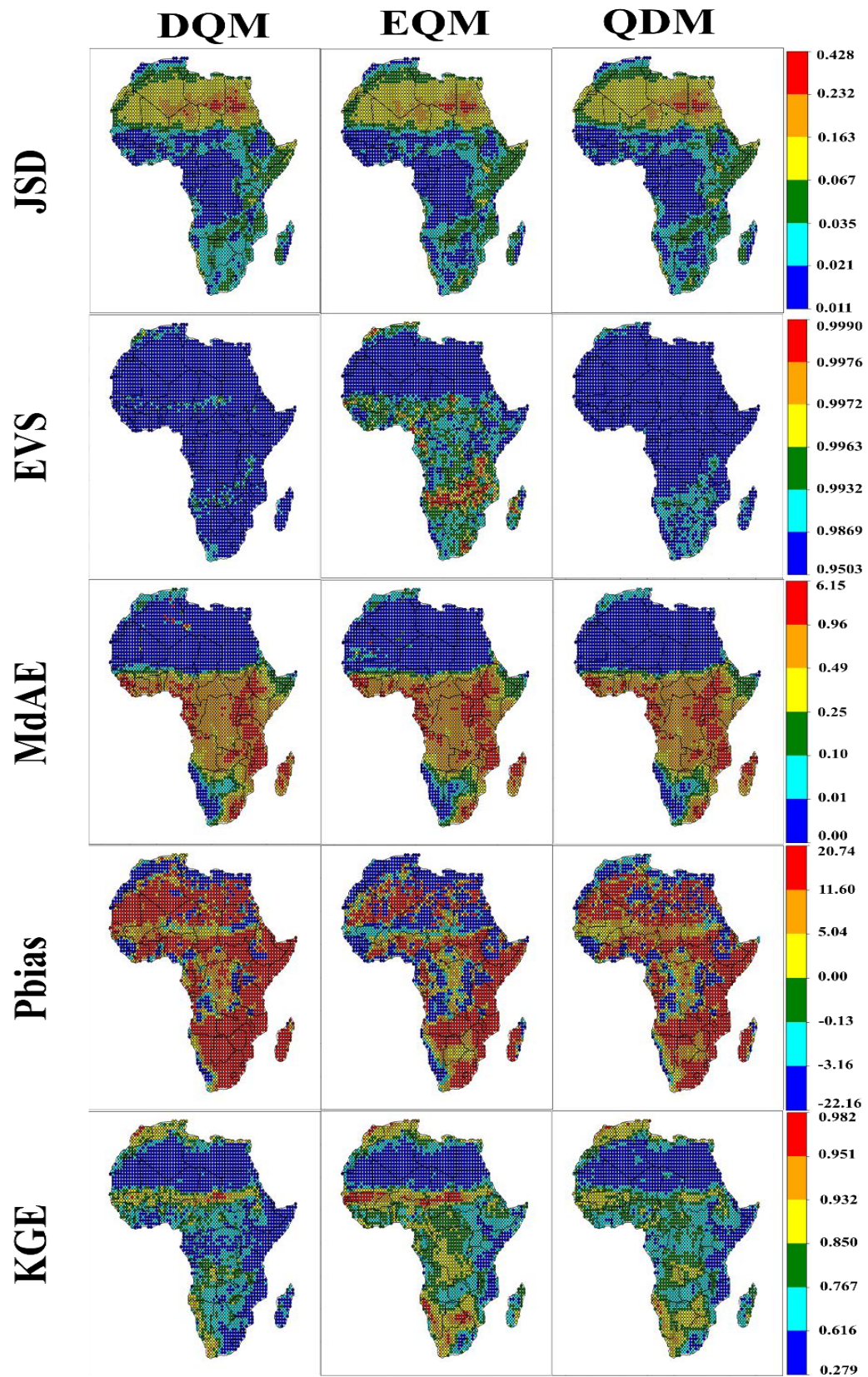
384



385
 386 Figure 3. Performance comparison of DQM, EQM, and QDM using evaluation metrics (MAE,
 387 MSLE, NSE, R^2 , and RMSE) for daily precipitation in North America.

388
 389 In this study, the daily precipitation in Africa was corrected using three QM methods, and the
 390 performance is shown in Figures 4 and S3. Overall, the JSD of precipitation corrected by the
 391 three methods showed similar spatial patterns, but the precipitation of DQM showed lower
 392 performance than the other methods in the southern region. In terms of EVS, the precipitation
 393 of DQM showed higher variability than the other methods. The precipitation of QDM showed

394 lower variability in southern Africa than DQM, but overall, it showed higher variability than
395 EQM. The precipitation of EQM showed lower variability in southern and central Africa but
396 still showed high variability in the northern region. Analyzing the error performance, the
397 precipitation corrected by QDM showed the best performance compared to the other methods.
398 In particular, QDM showed the highest performance in North Africa (MAE: 0.03, and MSLE:
399 0.004), and EQM's error performance was lower than QDM's in most indicators but better than
400 DQM's. Finally, EQM performed the highest in correlation metrics (NSE and R^2), and QDM
401 performed better than DQM.

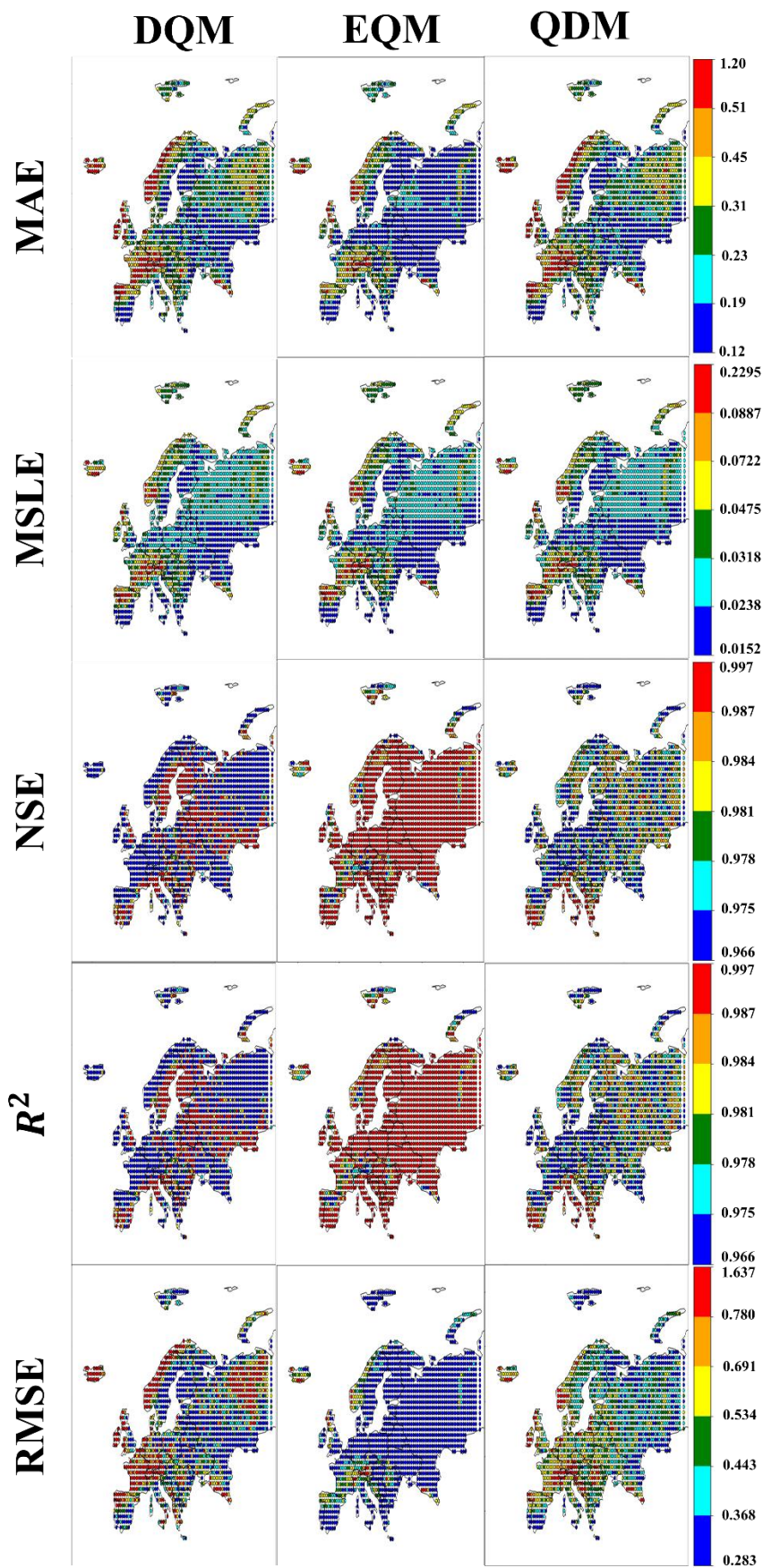


402

403 Figure 4. Performances of DQM, EQM, and QDM using evaluation metrics (JSD, EVS, MdAE,

404 Pbias, and KGE) for daily precipitation in Africa.

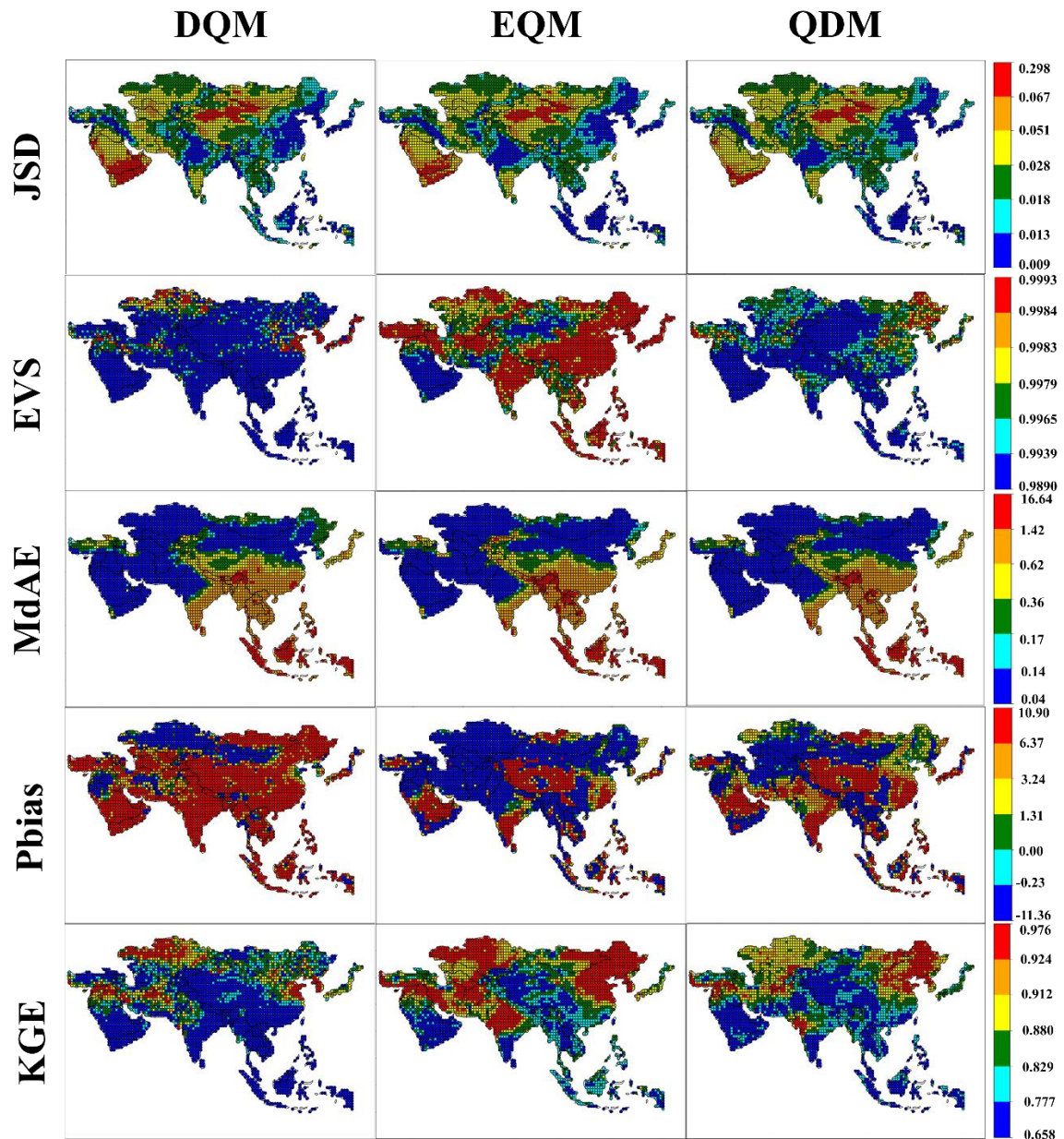
405 Figures 5 and S4 show the spatial results of the grid-based evaluation metrics for the European
406 region. In terms of error metrics, EQM-corrected precipitation performed the best across
407 Europe compared to other methods. In contrast, QDM-corrected precipitation performed
408 similarly to DQM in MAE and MSLE but significantly outperformed DQM in RMSE.
409 Regarding NSE and R, EVS, and KGE metrics, EQM-corrected precipitation performed
410 overwhelmingly better than other methods. QDM precipitation performed better than DQM,
411 while DQM performed the worst. Regarding Pbias, EQM-corrected precipitation was
412 underestimated compared to the reference data in most parts of Europe. In contrast, QDM-
413 corrected precipitation was more similar to the reference data compared to other methods, and
414 DQM precipitation was overestimated compared to the reference data except in central Europe.



416 Figure 5. Performances of DQM, EQM, and QDM using evaluation metrics (MAE, MSLE,
417 NSE, R^2 , and RMSE) for daily precipitation in Europe.

418 Figures 6 and S5 show the results of spatially quantifying the corrected precipitation in Asia
419 using various evaluation metrics. Regarding error metrics, EQM-corrected precipitation stands
420 out with its superior performance, particularly in RMSE, which was consistently below 1.35 in
421 most areas except for certain parts of Central Asia. In contrast, DQM-corrected precipitation
422 showed the poorest performance in error metrics. QDM-corrected precipitation demonstrated
423 a performance similar to EQM but slightly lower in East Asia and North Asia. In NSE and R,
424 the precipitation corrected by EQM performed better than other methods, especially in
425 Southwest and East Asia. In contrast, the precipitation corrected by DQM performed lower
426 than other methods. Regarding EVS, the precipitation corrected by EQM showed the lowest
427 variability, while QDM showed higher variability than EQM but lower variability than DQM.
428 In the case of Pbias, precipitation corrected by DQM was overestimated compared to the
429 reference data throughout Asia. The precipitation corrected by EQM was underestimated in
430 most regions except Central Asia. Precipitation in QDM showed a similar spatial pattern to that
431 in EQM, but the range of Pbias was more diverse.

432



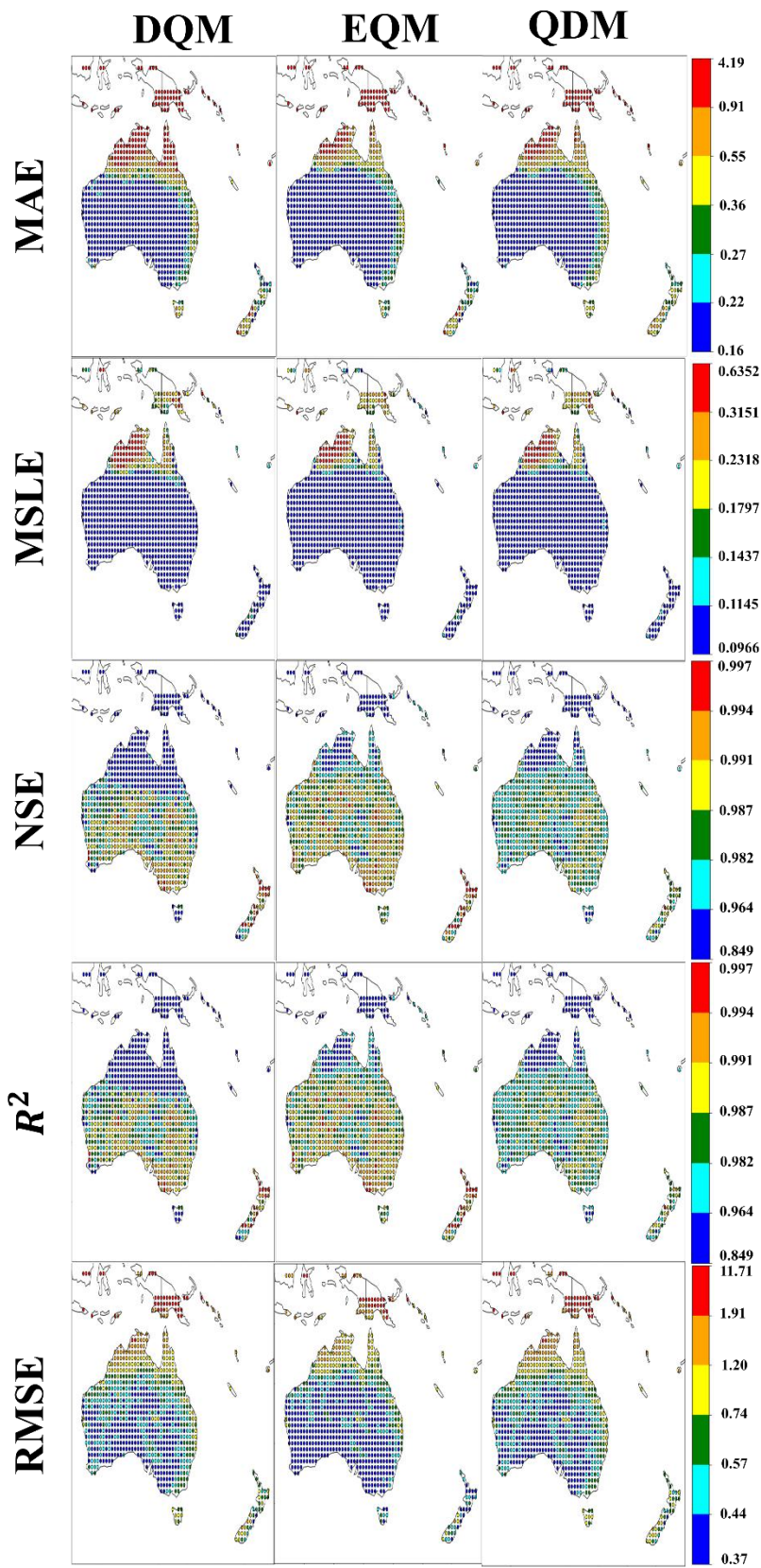
433

434 Figure 6. Performances of DQM, EQM, and QDM using evaluation metrics (JSD, EVS, MdAE,
 435 Pbias, and KGE) for daily precipitation in Asia.

436

437 Figures 7 and S6 show the results of spatially quantifying the corrected daily precipitation in
 438 Oceania using various evaluation metrics. In terms of error metrics, the precipitation estimated
 439 by the three QM methods performed similarly in MAE, MdAE, and MSLE. However, the
 440 precipitation corrected by EQM performed better in RMSE than the other methods. In the case
 441 of JSD, all three methods performed well.

442 Regarding EVS, the precipitation corrected by EQM showed lower variability than the other
443 methods, and DQM showed higher performance than QDM. In Pbias, the precipitation adjusted
444 by QDM was overestimated compared to the reference data in Oceania, while the precipitation
445 corrected by DQM and EQM was underestimated compared to the reference data in central and
446 southern Oceania. Finally, in KGE, precipitation corrected by EQM showed the highest
447 performance, while DQM showed the lowest.



448

449 Figure 7. Performances of DQM, EQM, and QDM using evaluation metrics (MAE, MSLE,

450 NSE, R^2 , and RMSE) for daily precipitation in Oceania.

451 Figure 8 visualizes the results of evaluating the bias-corrected precipitation data using 11
452 CMIP6 GCMs on six continents using ten evaluation metrics as boxplots. Overall, the
453 precipitation corrected by EQM outperforms the other methods on most continents. In
454 particular, EQM performs the best on the error metrics. QDM performs slightly lower than
455 EQM but still maintains a high level of performance on all continents. On the other hand, DQM
456 has more significant errors and relatively poor performance compared to the other methods on
457 most metrics.



(a) South America (b) North America (c) Africa (d) Europe (e) Asia (f) Oceania

458

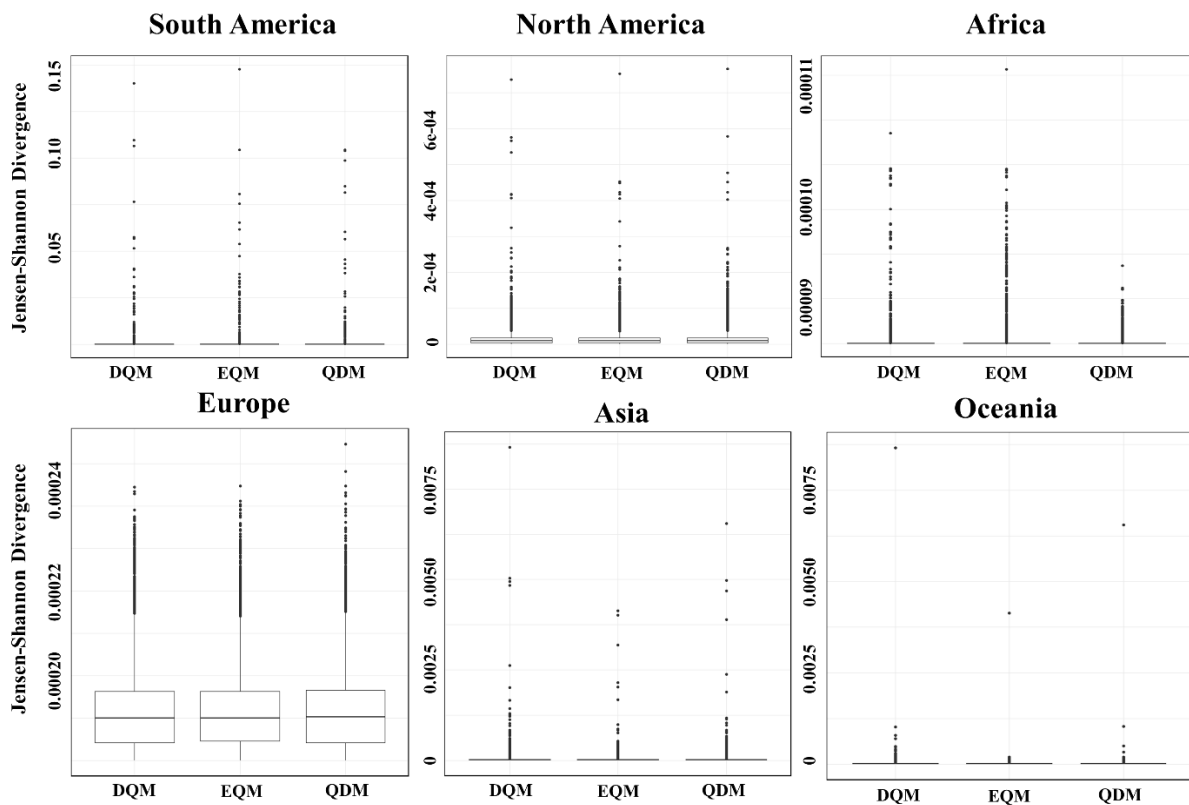
459 Figure 8. Performances of DQM, EQM, and QDM of historical period precipitation using

460 boxplots based on ten evaluation metrics

461

462 **3.1.3 Comparison of reproducibility for extreme daily precipitation**

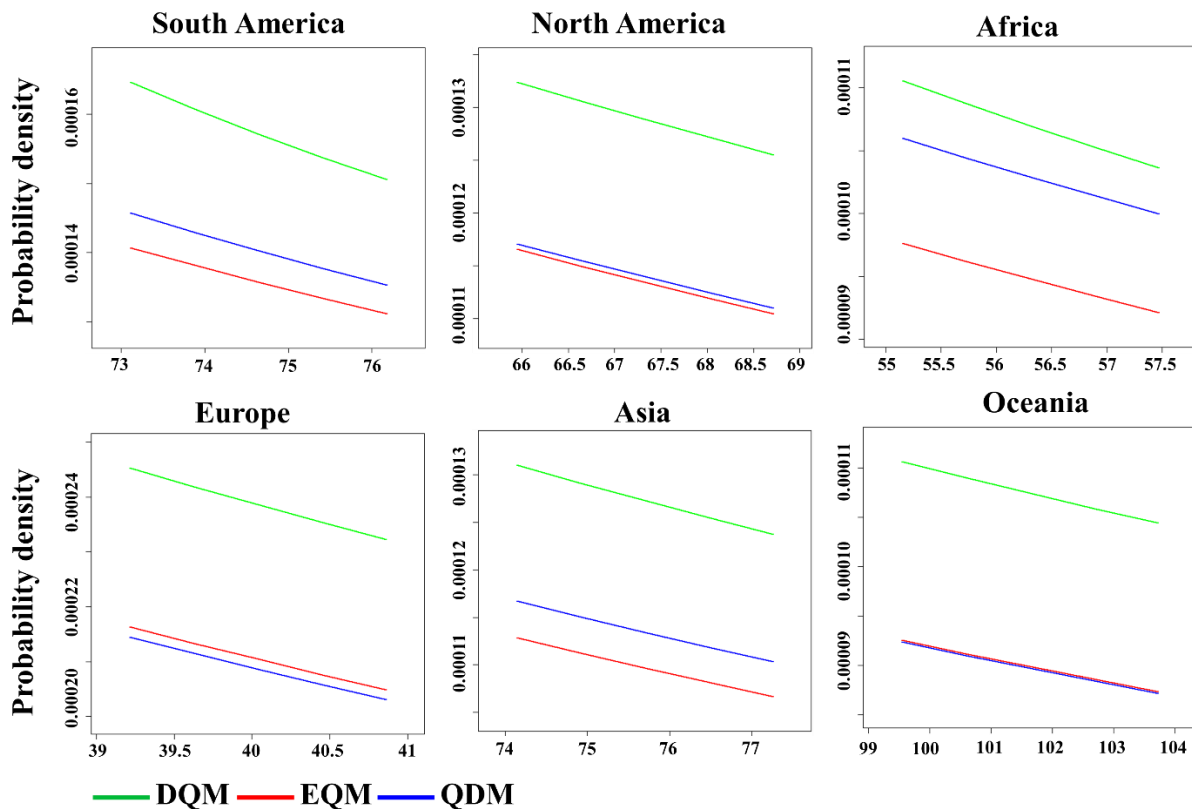
463 This study compared the daily extreme precipitation corrected by three methods using the GEV
464 distribution. **Figure 9 compares the distribution differences of the daily precipitation adjusted**
465 **by the bias correction methods based on the GEV distribution using the JSD.** In general, the
466 JSD values for precipitation from DQM, EQM, and QDM are very low for most continents,
467 indicating that the GEV distributions are almost identical among the three methods. Although
468 there are some outliers, the overall distribution differences are not significant, suggesting little
469 difference among the three methods when correcting for historical precipitation. However, in
470 Europe, unlike other continents, the differences between the first and third quartiles of the JSD
471 are relatively significant, indicating that the distributions can vary significantly from grid
472 grid depending on the QM method.
473



474
475 Figure 9. Comparison of distribution differences for GEV distribution using JSD across six
476 continents.

477
478 Figure 10 shows the probability density functions for extreme precipitation above the 95th
479 percentile of the GEV distribution. Overall, DQM shows the highest probability density for

480 extreme precipitation across all continents and has the widest distribution, indicating that DQM
 481 corrects more extreme precipitation. On the other hand, EQM shows the lowest probability
 482 density and conservatively corrects for extreme precipitation. QDM shows probability
 483 densities between EQM and DQM across most continents but closer to EQM.



484
 485 Figure 10. Comparison of probability densities for extreme precipitation values above the 95th
 486 percentile using GEV.

487
 488 **3.2 Prioritization of bias correction methods based on performance**

489 **3.2.1 Results of weight for evaluation metrics**

490 In this study, the weights were calculated by applying entropy theory to the evaluation metrics
 491 used in the TOPSIS analysis, and the results are presented in Table 3. JSD had the highest
 492 weight in South America because the estimated JSD from 11 CMIP6 GCMs was an important
 493 metric for evaluating model performance differences. These results indicate that the differences
 494 between distributions are significant. On the other hand, EVS and NSE in South America had
 495 very low weights, suggesting that the variability and efficiency of precipitation were considered
 496 less important than other indicators. For North America, the RMSE, MSLE, and MAE metrics
 497 were of significant importance, as evidenced by their high weights. These error metrics

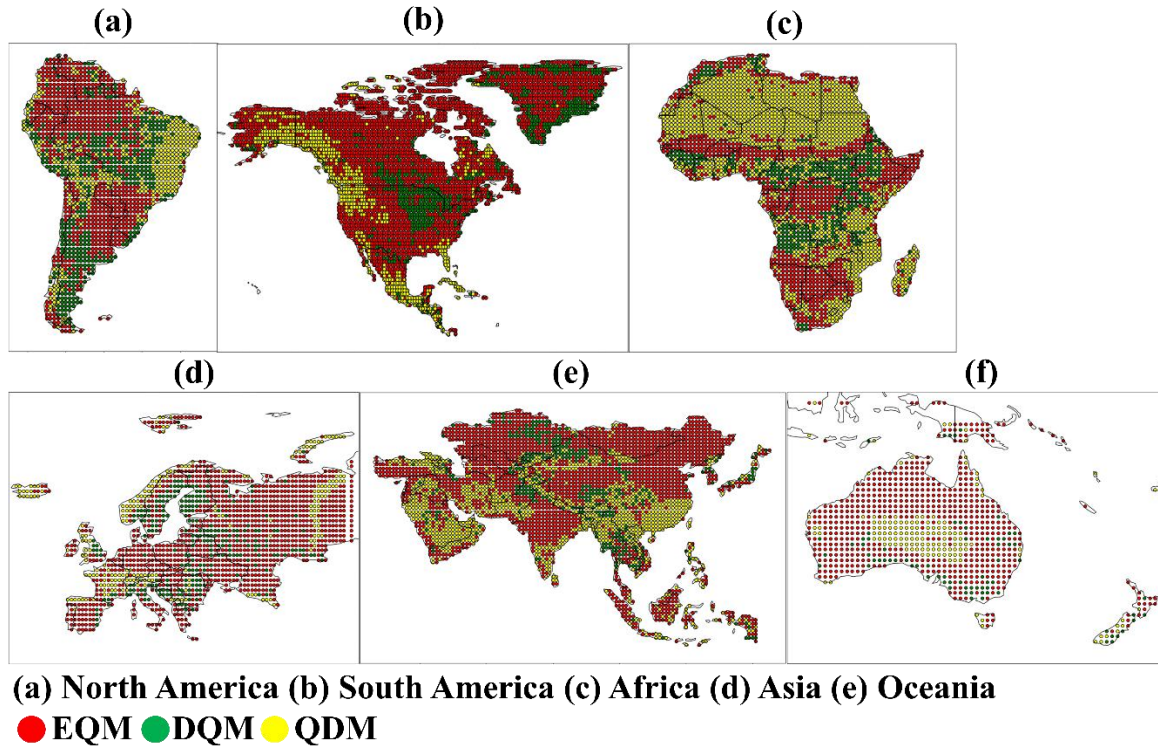
498 revealed substantial regional differences. In contrast, EVS carried a negligible weight,
 499 suggesting it was less important in explaining variability in North America. For Africa, MdAE
 500 and JSD metrics were of considerable importance, as indicated by their high weights. These
 501 metrics were key evaluation factors in Africa. Conversely, EVS carried a low weight,
 502 suggesting it was considered relatively less important. RMSE had the highest weight in Europe,
 503 and KGE also had a relatively high weight, indicating that these metrics were considered
 504 important evaluation criteria in Europe. In Asia, MAE and MSLE had high weights, suggesting
 505 that these metrics were important evaluation metrics. On the other hand, EVS and NSE were
 506 considered less important due to their low variability. **In Oceania, high weights were assigned**
 507 **to JSD, KGE, RMSE, and MAE, suggesting that these metrics are critical for evaluating model**
 508 **performance.** On the other hand, R^2 and NSE were assigned low weights.

509
 510 Table 3. Entropy-based weights for evaluation metrics across different continents

	RMS E	MAE	R^2	NSE	KGE	Pbias	MdAE	MSLE	EVS	JSD
South America	0.1439	0.1536	0.0001	0.0001	0.0005	0.0238	0.1754	0.1934	0.0004	0.3088
North America	0.2289	0.1908	0.0001	0.0001	0.0007	0.0118	0.2152	0.2117	0.0001	0.1411
Africa	0.1319	0.1686	0.0002	0.0002	0.0002	0.0855	0.2436	0.1911	0.0002	0.1786
Europe	0.2821	0.1762	0.0022	0.0022	0.0063	0.0378	0.1754	0.1666	0.0021	0.1490
Asia	0.2073	0.1954	0.00003	0.00003	0.0001	0.0305	0.2300	0.2024	0.00003	0.1342
Oceania	0.2384	0.2204	0.0013	0.0013	0.0068	0.0214	0.2338	0.2093	0.0012	0.0660

511
 512 **3.2.2 Selection of the best bias correction method based on TOPSIS**
 513 Figures 11 and S7 present the best bias correction method selected for each continent using the
 514 TOPSIS approach. In Figure 11(a), the spatial distribution of the most effective bias correction
 515 method across the grid points of each continent is shown. In contrast, Figure 11(b) shows the
 516 number of grid points selected for each QM method. In South America, EQM was chosen as
 517 the best method in most grid points, with EQM being selected in over 1,500 grid points. In
 518 contrast, QDM was selected in fewer than 700 grid cells, making it the least chosen method in
 519 South America. Across all continents except South America, EQM was selected as the best
 520 model in the majority of grid cells, with the number of selected grid points (North America:
 521 7,583; Africa: 2,879; Europe: 2,719; Asia: 8,793; and Oceania: 1,659). On the other hand,

522 DQM was the least chosen method across all continents. For QDM, although it was the second
 523 most selected method across all continents except South America, the difference in the number
 524 of grid points between QDM and EQM is significant.



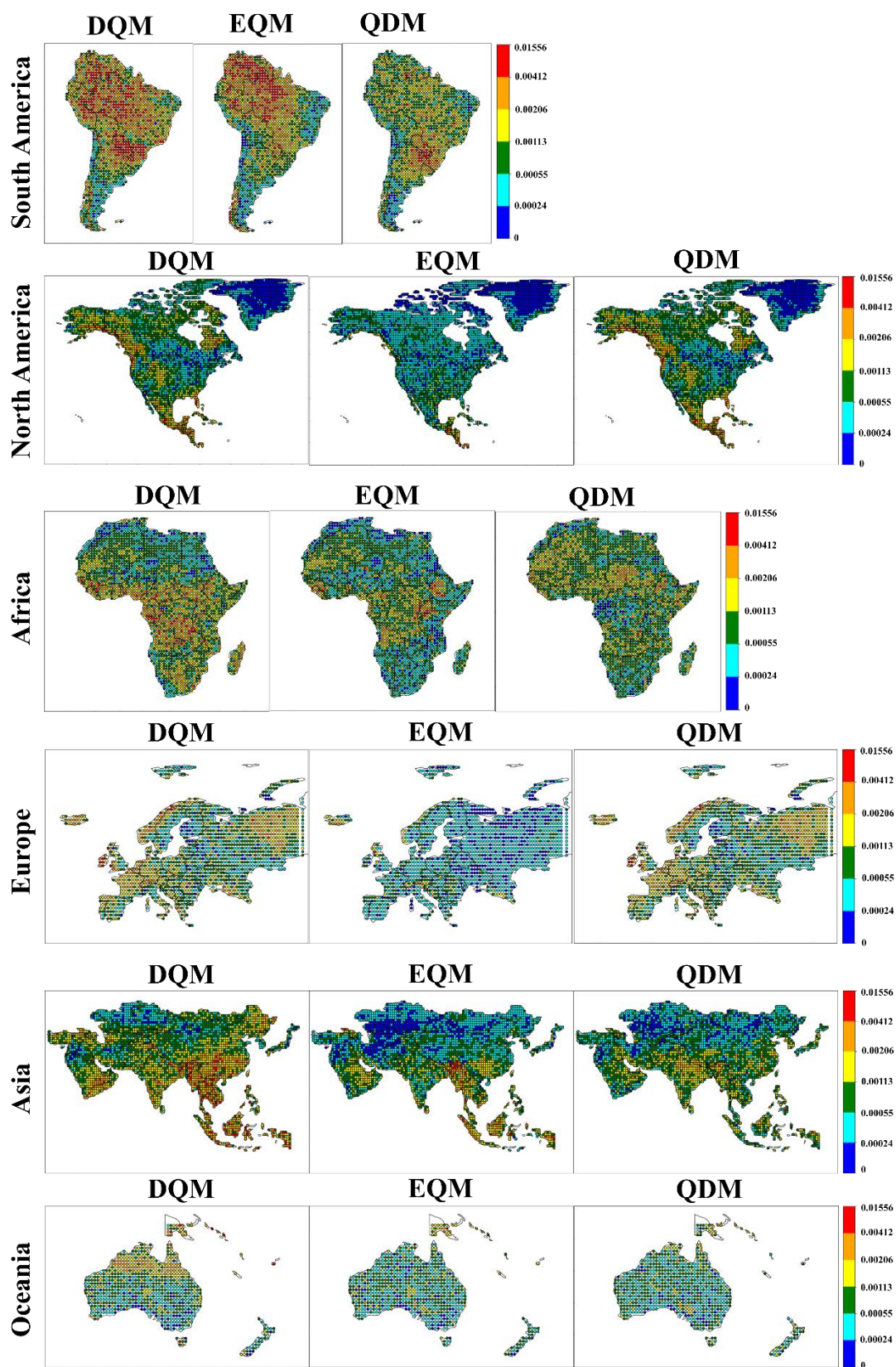
525
 526 Figure 11 Spatial distribution for selected best bias correction methods across continents
 527 using TOPSIS

529 3.3 Uncertainty quantification of bias corrected daily precipitation

530 3.3.1 Uncertainty by model

531 This study quantifies the daily precipitation uncertainty of 11 CMIP6 GCMs, corrected using
 532 three different BMA methods. Figure 12 shows the distribution of GCM weight variances
 533 calculated by BMA across six continents. In South America, the highest weight variance was
 534 observed mainly in DQM. EQM showed high weight variance in the northern region but lower
 535 variance than DQM in most other regions. QDM exhibited the lowest weight variance, with
 536 values less than 0.00113 in most regions. In North America, EQM had the lowest weight
 537 variance, with values between 0.00055 and 0.00024 in most regions. QDM showed the lowest
 538 model uncertainty across North America, with more regions where weight variances were
 539 closer to 0 than the other methods. On the other hand, DQM exhibited high weight variance
 540 overall, with exceptionally high model uncertainty in the northeast and southern regions. In

541 Africa, EQM's weight variance was estimated to be low overall, resulting in low model
542 uncertainty in most regions. For QDM, weight variance was low in some regions but higher
543 than 0.00113 in others. DQM showed high weight variance in most regions except for the
544 northern area, indicating high model uncertainty across the continent. EQM's weight variance
545 was the lowest in Europe compared to the other methods, with weight variances close to 0
546 across the continent. QDM also showed low weight variance overall, though higher than EQM.
547 DQM exhibited high weight variance in most regions except for Central Europe. In Asia, EQM
548 showed low weight variance in most regions except Southeast Asia. QDM's weight variance
549 was similar to EQM's, though some regions had higher model uncertainty. DQM showed high
550 weight variance in most regions except for some Southwest and North Asian areas. For Oceania,
551 the weight variances of EQM and DQM were mainly similar, but DQM showed a higher weight
552 variance overall.

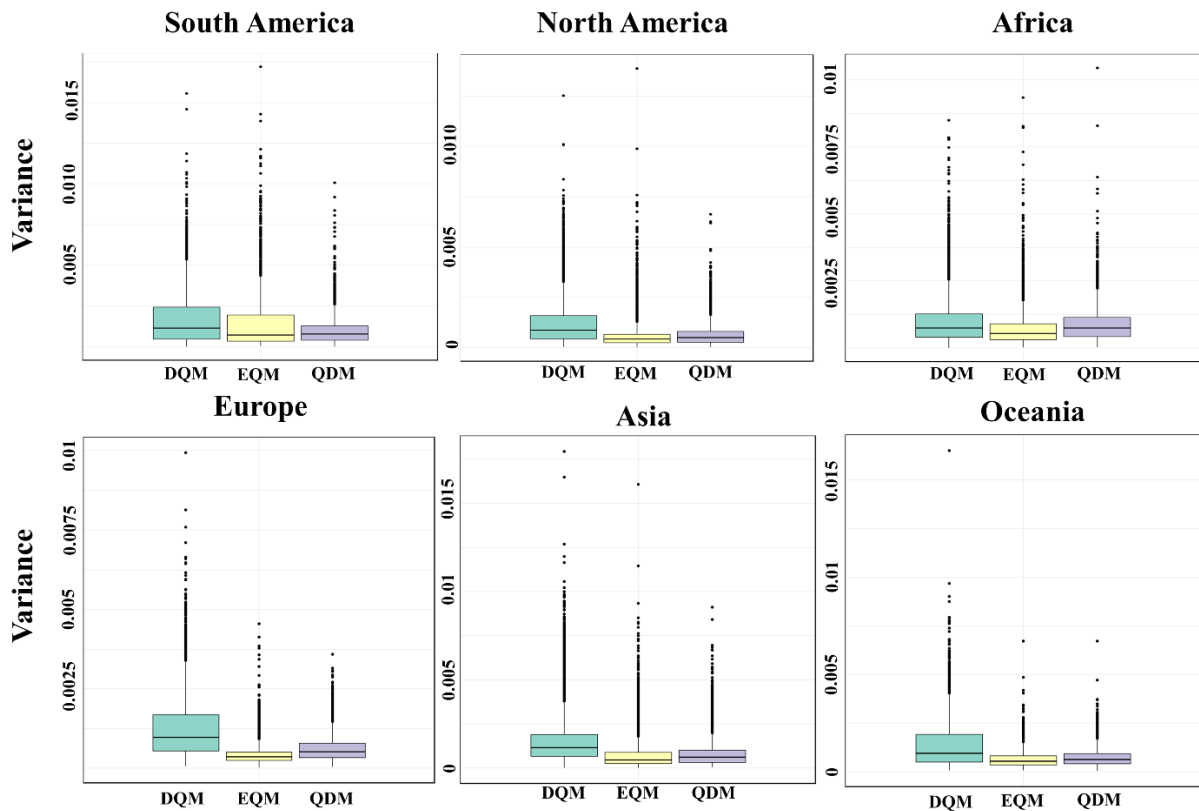


553

554 Figure 12. Spatial distribution of weight variance across continents for bias corrected CMIP6

555 GCMs using BMA

556 Figure 13 shows the distribution of GCM weight variances calculated using BMA across six
 557 continents, presented as boxplots. Overall, EQM has the smallest weight variance, and QDM
 558 has the second smallest weight variance on all continents except South America. In contrast,
 559 in South America, QDM has the smallest weight variance, and EQM has the second smallest.
 560 DQM consistently has the largest weight variance across all continents, indicating the highest
 561 model uncertainty.
 562

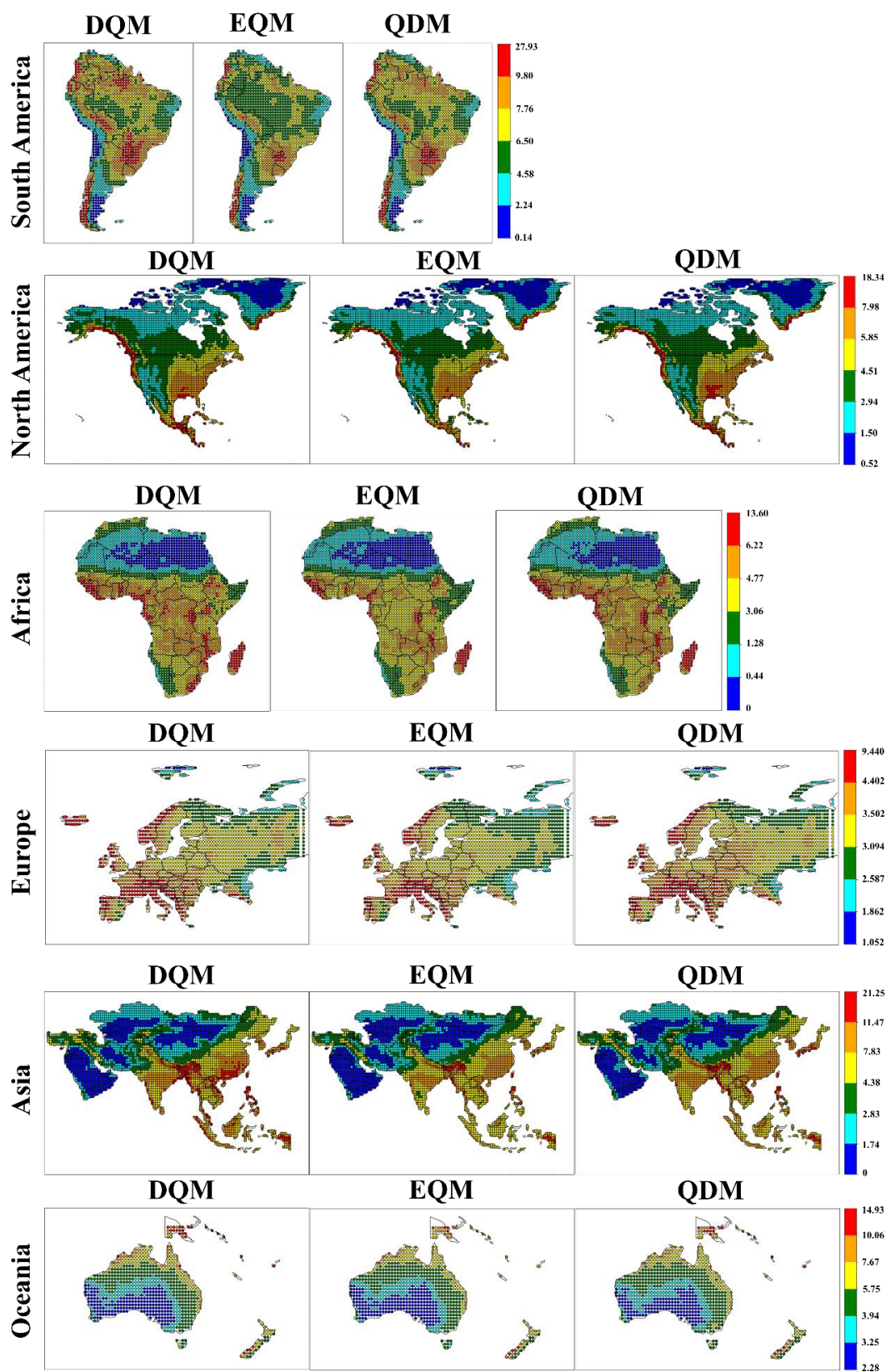


563
 564 Figure 13. Weight variance for bias correction methods across six continents using box plots.
 565

566 3.3.2 Uncertainty by ensemble prediction

567 A daily precipitation ensemble for the historical period was generated using BMA on 11
 568 CMIP6 GCMs, and the standard deviation of daily precipitation by continent is presented as
 569 shown in Figure 14. Overall, the ensemble predicted using EQM provided stable precipitation
 570 projection with low standard deviations across most continents. The QDM ensemble showed
 571 similar results to EQM for most continents except Oceania, but the standard deviations were
 572 slightly higher. On the other hand, the ensemble using DQM exhibited higher standard
 573 deviations than the other methods for all continents and had the largest prediction uncertainty.

574 In Oceania, the ensembles predicted by the three methods showed similar results. However,
575 the prediction uncertainty was estimated to be lower in the order of EQM, DQM, and QDM
576 due to slight differences.



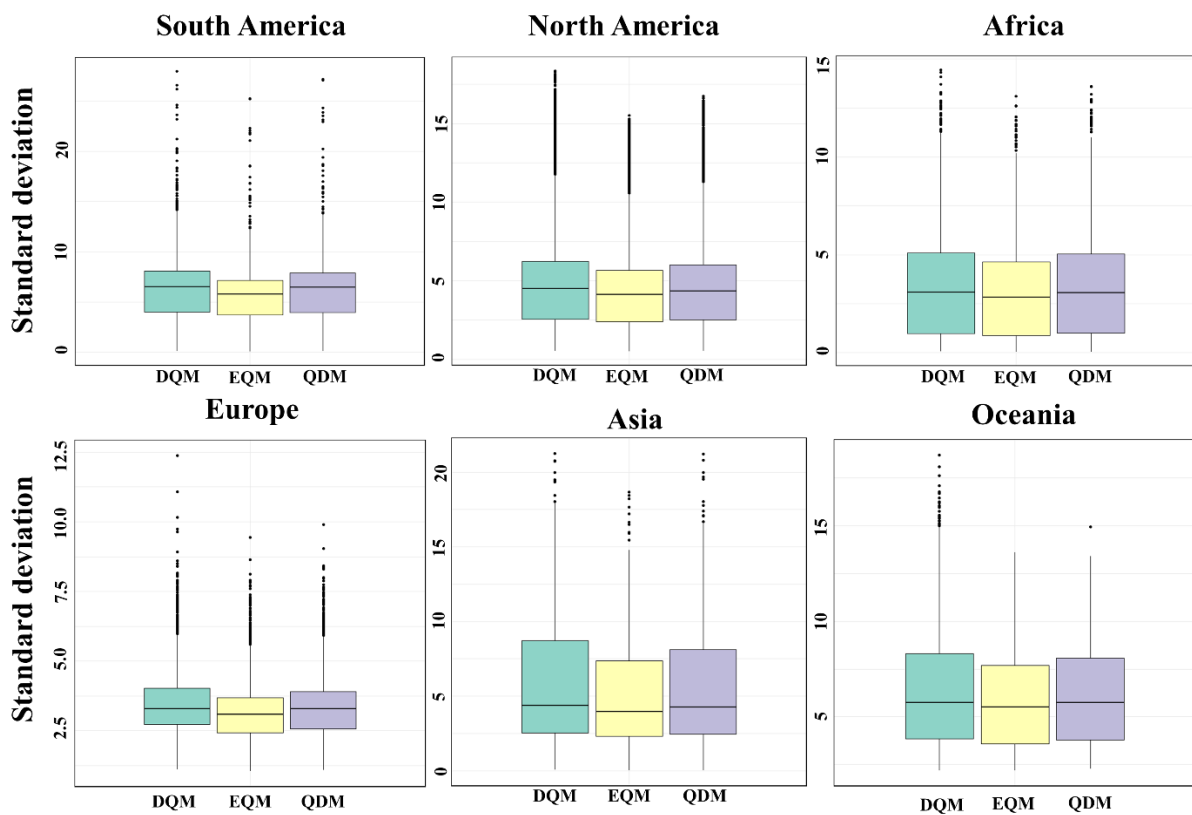
577

578 Figure 14. Spatial distribution of standard deviation for daily precipitation across continents

579 for bias corrected CMIP6 GCMs using BMA

580
581
582
583
584
585
586
587
588

Figure 15 shows the standard deviation of daily precipitation for the ensemble forecasted by BMA using three methods, DQM, EQM, and QDM, in a boxplot for each continent. Overall, the EQM ensemble showed the lowest standard deviation across all continents, providing the most stable daily precipitation forecasts. The QDM ensemble showed slightly higher standard deviations than EQM for most continents, but there was no significant difference between the two methods. In contrast, the DQM ensemble showed the highest standard deviation and the largest prediction uncertainty.



589
590
591
592

Figure 15. Spatial distribution of standard deviation for daily precipitation across continents for bias corrected CMIP6 GCMs using BMA

593 3.4 Evaluation of bias correction methods using CI

594 3.4.1 Results of CI by each weighting case

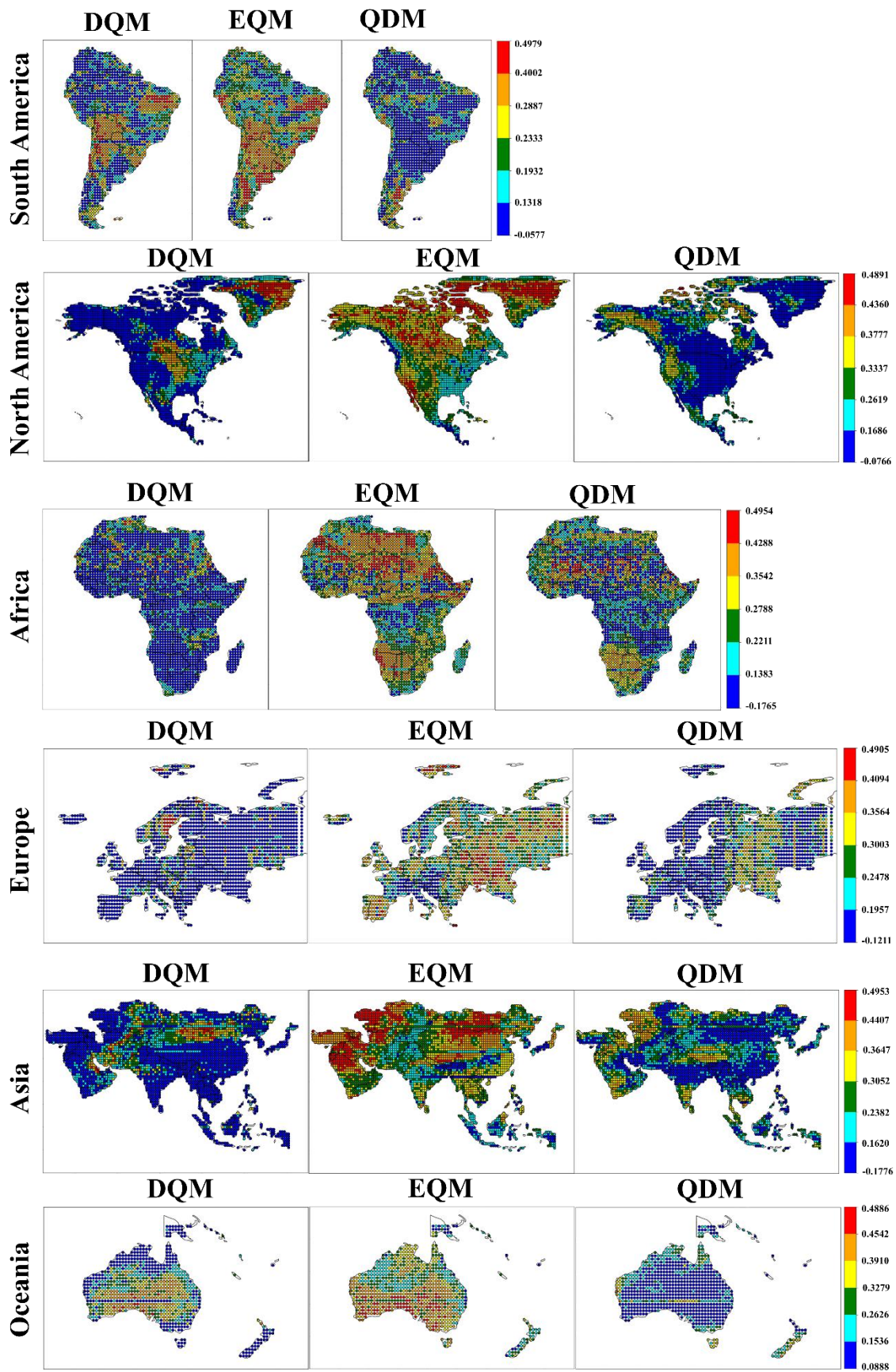
595 This study compared three QM methods by generating a CI based on three cases of weighting
596 values that considered both model performance and uncertainty. Figures 16, S8, and S9 show

597 the comprehensive indices calculated by applying equal weights and weights emphasizing
598 performance and uncertainty, respectively.

599 EQM showed the highest CI across all continents when equal weights were applied. However,
600 the index was lower in southern Europe and southeastern North America, but it calculated high
601 values in most other regions. QDM showed high index values in some regions, although they
602 were lower than those of EQM. For example, the CI results were high in the northern and
603 western parts of North America and the central part of Europe. On the other hand, DQM was
604 generally unsuitable in most regions but showed a relatively high index in Oceania.

605 When weights that emphasized performance were applied, DQM showed a high index in the
606 central part of South America but low performance in most continents. Nevertheless, DQM
607 showed a better index than QDM in some parts of Oceania. EQM showed the best index across
608 most continents. While QDM was less suitable than EQM, it was still evaluated as a useful
609 method in some continents.

610 Even when applying weights that increased the emphasis on uncertainty, similar results were
611 obtained with the other weighting values. In particular, EQM was evaluated as the most suitable
612 model across all continents, while DQM showed the opposite results.

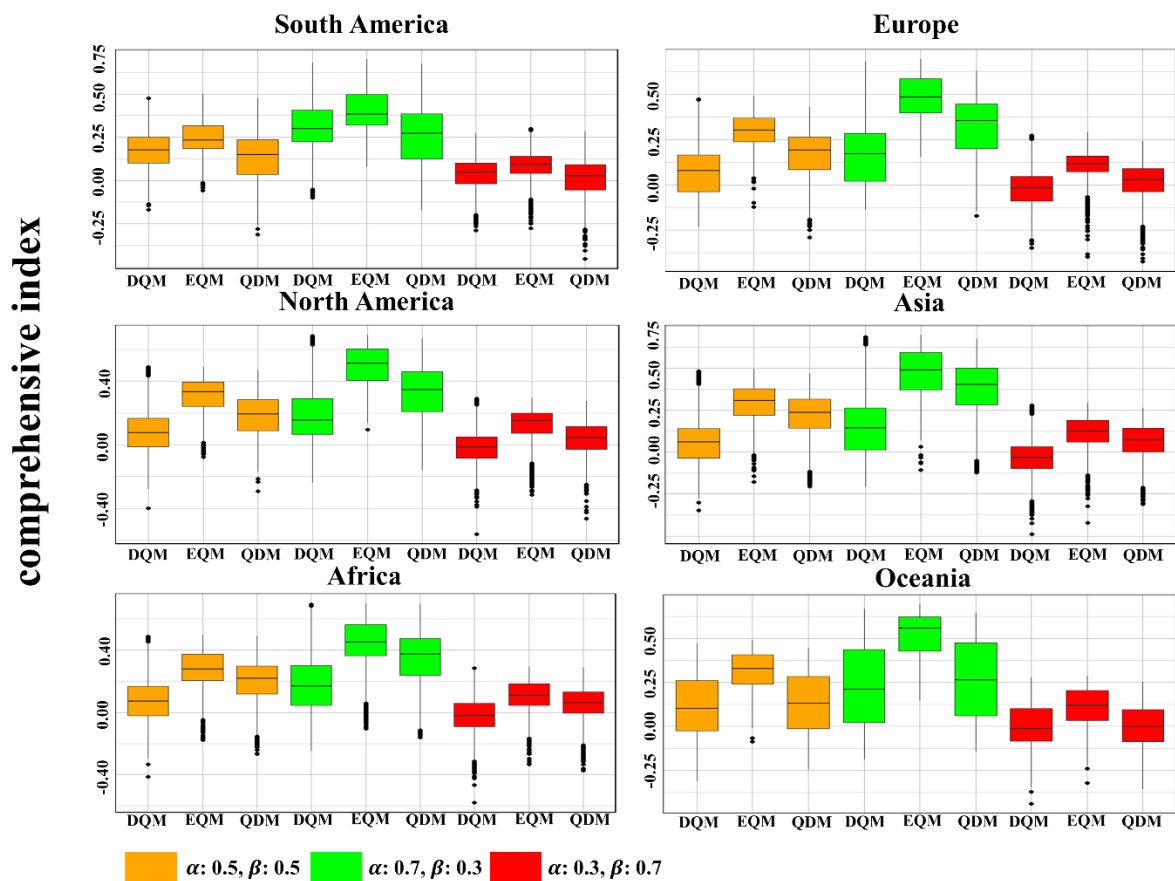


614 Figure 16. Spatial distribution of comprehensive indices for bias correction methods with equal
 615 weights ($\alpha: 0.5, \beta: 0.5$) across continents

616

617 Figure 17 presents a comparison of the comprehensive indices for three QM methods with
 618 different weights for each continent using box plots. Overall, all methods showed higher
 619 indices than the other weighting values in the values that emphasized more weight on
 620 performance. In all weighted values, DQM showed the lowest indices in all continents except
 621 for South America and Oceania, where it was slightly higher or similar to QDM. EQM showed
 622 the best composite indices in all continents, outperforming performance and uncertainty. QDM
 623 showed high comprehensive indices in most continents, and the gap with EQM narrowed
 624 significantly in the weighting values that emphasized performance more. Nevertheless, QDM
 625 overall had lower comprehensive indices than EQM.

626



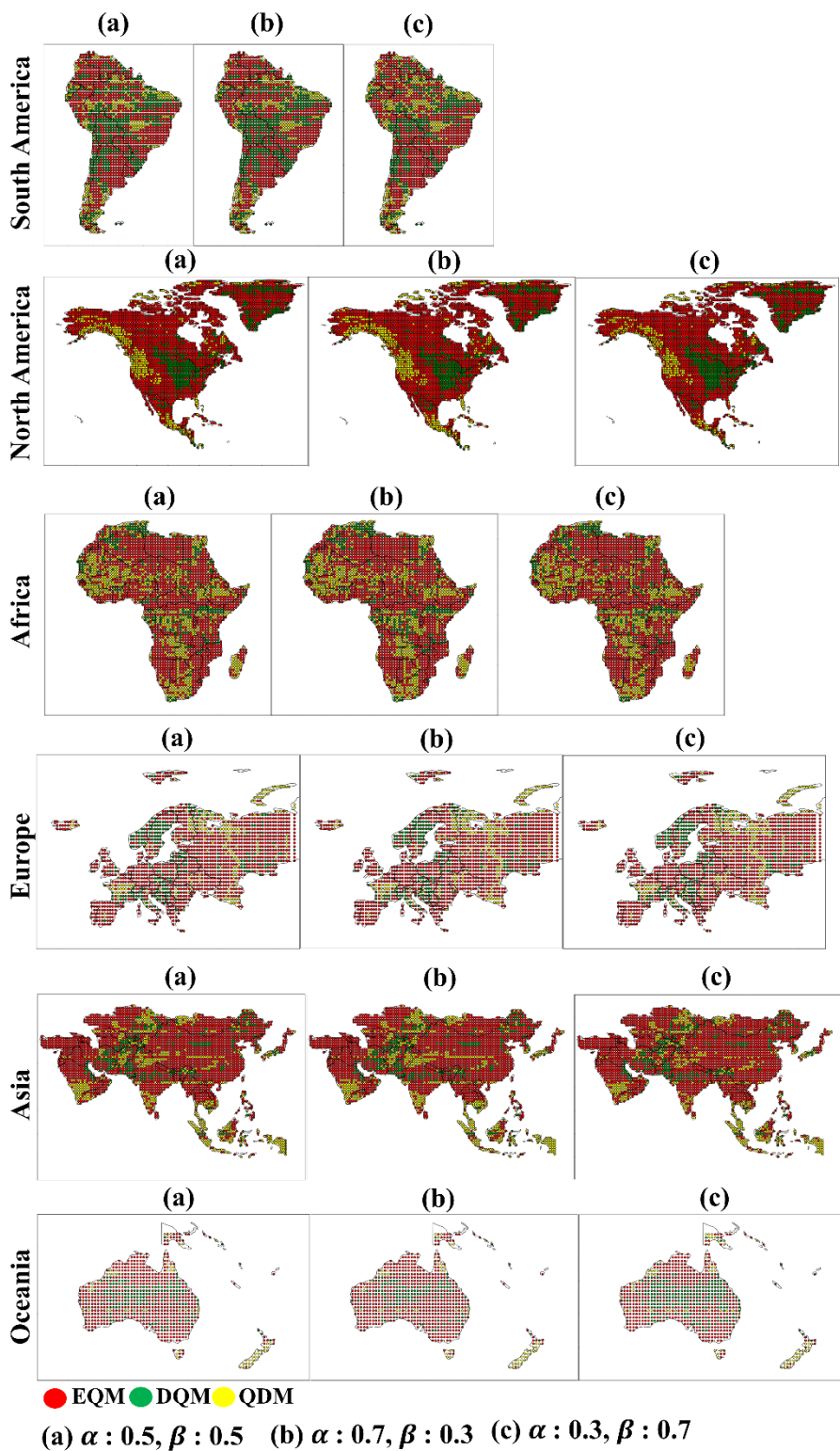
627

628 Figure 17. CI for three bias correction methods across continents with varying weights on
 629 performance and uncertainty

630

631 **3.4.2 Selection of best bias correction method**

632 Based on the CI, this study selected the best bias correction method for each continent. Figure
633 18 shows how the best bias correction method was selected for each continent by applying
634 various weighting values of the CI. Overall, EQM was selected as the best correction method
635 for most continents in all weighting values and was selected more than other methods in North
636 America, Europe, Asia, and Oceania. DQM was selected the least in most continents except
637 for South America and Oceania, and the number of selected grids tended to decrease as the
638 weighting for uncertainty increased. **QDM was selected as the best bias correction method in**
639 **western North America, southern and eastern Africa, and northern Europe.** In addition, QDM
640 was selected the most in Southeast Asia in all weighting values.



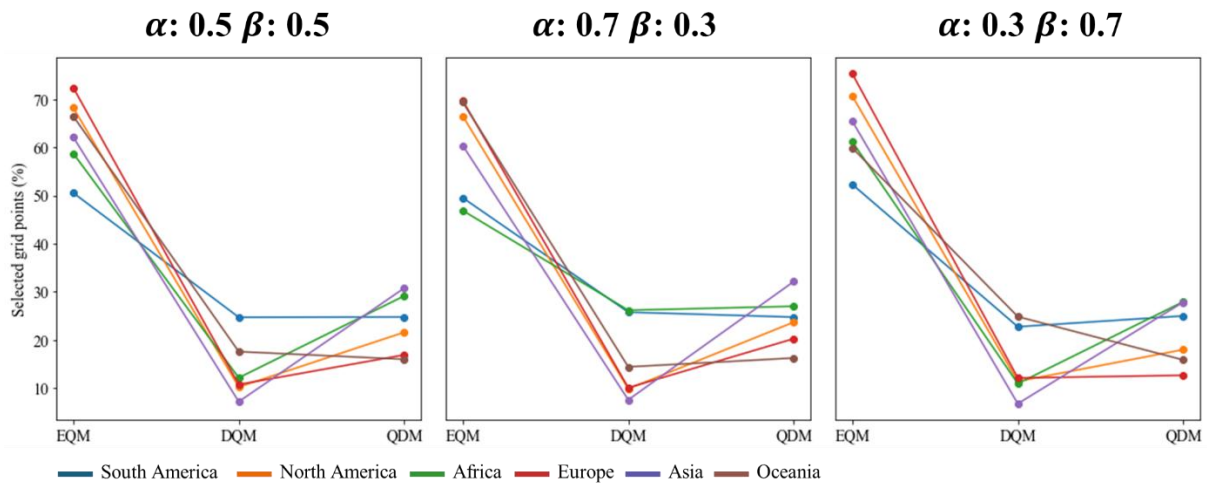
641

642 Figure 18. Selection of best bias correction methods across continents based on CI depending

643 on weighting values.

644

645 Figure 19 shows the number of selected grids for the best bias correction method across
 646 continents based on three weighting values. Overall, EQM was the most frequently selected
 647 method across all weighting values, demonstrating superior performance across all continents
 648 compared to the other methods. Interestingly, as the weight for uncertainty increased, the
 649 number of grids where EQM was selected also increased, while the number decreased as the
 650 weight for performance increased. In contrast, QDM was chosen as the second-best method on
 651 most continents, except for South America and Oceania. The number of selected grids for
 652 QDM slightly increased as the performance weight increased. DQM was the least selected
 653 method across most continents, indicating that it was the least suitable overall.
 654



655
 656 Figure 19. Ratios of selected grids for best bias correction methods across continents based on
 657 different weighting values
 658

659 4. Discussion

660 Bias correction methods are widely used in correcting GCM outputs, and previous studies have
 661 compared the performance of various methods (Homsí et al., 2019; Saranya and Vinish, 2021).
 662 Among these, Quantile Mapping (QM) has consistently shown superior performance compared
 663 to other methods, making it a widely used approach for bias correction. In particular, QDM,
 664 EQM, and DQM, which are the focus of this study, are frequently employed in research
 665 exploring and applying climate change projections based on GCM outputs (Cannon et al., 2015;
 666 Switanek et al., 2016; Song et al., 2022a). Analyzing the strengths and limitations of these three
 667 methods will provide valuable insights for climate researchers, enabling them to choose the
 668 most suitable bias correction method for specific regions. In this context, this study further

669 evaluates the performance of QDM, EQM, and DQM, especially for daily precipitation, and
670 investigates how these methods perform across different regions. Unlike previous studies that
671 focused on the performance of bias correction methods (Song et al., 2024a; Teutschbein and
672 Seibert, 2012; Smitha et al., 2018), this study suggests a CI that integrates the performance and
673 uncertainty metrics. This approach enhances the robustness of bias correction method selection
674 and provides a more holistic evaluation framework. This section discusses the strengths and
675 weaknesses of each method from various perspectives to provide a more balanced assessment.
676

677 **4.1 Evaluation of bias correction methods performance**

678 The daily precipitation corrected by the three QM methods outperformed the raw GCM data
679 (see Figure 1). **All three methods, as evidenced by the Taylor diagram, demonstrated overall
680 stronger performance than the raw GCM and consistently produced good results across various
681 regions. Nonetheless, the performance of the bias-corrected GCMs clearly differs. This
682 highlights the need to use multiple performance metrics to fully understand the strengths and
683 weaknesses of the three QM methods, as relying on a single analysis or macroscopic
684 perspective can overlook important details.** From this perspective, many studies have
685 emphasized the application of a multifaceted analysis in selecting bias correction methods
686 (Homsí et al., 2019; Cannon et al., 2015; Berg et al., 2022; Song et al., 2023). The spatial
687 distribution of correction performance, as discussed in Section 3.1.2, varies significantly by
688 continent. Figures 2 to 7 reveal that the evaluated metrics differ across continents, underscoring
689 the importance of region-specific correction methods. This finding aligns with Song et al.
690 (2023), highlighting the importance of selecting appropriate correction methods based on the
691 precipitation distribution at observation sites. Moreover, studies such as Homsí et al. (2019)
692 and Saranya and Vinish (2021) also emphasize the variability in bias correction performance
693 depending on the regional climate and data characteristics, reinforcing the need for tailored
694 approaches. Of course, the three QM methods showed high performance across most continents,
695 effectively correcting the biases in daily precipitation from GCMs. However, the corrected
696 daily precipitation varies subtly among the three methods, with these differences becoming
697 more pronounced in extreme events or specific evaluation metrics. For example, the three QM
698 methods tend to perform less effectively in regions with high precipitation, but their
699 performance also varies by grid (e.g., southern India in Asia: RMSE; central Oceania: Pbias
700 and EVS; central Europe: Pbias, MdAE, and KGE). While EQM performs well across most

701 continents, DQM and QDM show superior results in specific regions. Similar results were
702 made by Cannon et al. (2015), which highlighted differences in the performance of bias
703 correction methods, particularly in handling extreme precipitation events. QDM's error-related
704 metrics (South America: RMSE, MAE, and MSLE) are nearly identical to EQM's, yet QDM
705 outperforms EQM regarding MDAE on more grids. These findings suggest that a more nuanced
706 and detailed analysis of precipitation corrected by GCMs is necessary, aligning with the
707 conclusions of Gudmundsson et al. (2012), which emphasize that the effectiveness of bias
708 correction methods can vary significantly depending on local climate characteristics,
709 highlighting the importance of selecting appropriate methods for each region. These results
710 suggest a more detailed precipitation analysis from corrected GCMs is needed.

711 This study compared the three QM methods for daily precipitation events above the 95th
712 percentile (extreme precipitation) using the GEV distribution, as shown in Figure 10. The
713 results indicate that DQM tends to correct more extreme precipitation events than QDM,
714 aligning with previous findings that DQM captures a broader range of extremes. The unique
715 characteristics of DQM caused these results. DQM overestimated the corrected extreme
716 precipitation due to the relative variability in the data introduced through detrending, and the
717 subsequent reintroduction of the long-term mean during the correction step widened the range
718 of extreme precipitation, leading to overestimation compared to the reference data in areas with
719 high variability. At the same time, QDM and EQM take a more conservative approach (as noted
720 in previous studies such as Cannon et al., 2015). These findings suggest that EQM and QDM
721 may be more suitable in regions vulnerable to floods and extreme weather events that require
722 a more balanced and cautious approach. However, when comparing the differences in GEV
723 distributions, there was no significant difference between methods in regions like Oceania and
724 Europe (see Figure 9). These results imply that EQM can better handle extreme values or
725 outliers in the data by directly comparing and correcting past and future distributions. In
726 particular, EQM is consistent with previous studies in that it more accurately corrects observed
727 distributions in non-stationary and highly variable climate variables, such as precipitation
728 (Thiemeßl et al., 2012; Maraun, 2013; Gudmundsson et al., 2012). These positive aspects are
729 mainly due to EQM's ability to align the empirical ECDFs of reference and model data across
730 all quantiles, allowing it to correct biases with high precision at both central tendencies and
731 extremes. Although there are significant advantages in observing the results of the correction
732 method in detail from various perspectives, presenting these results without integrating them

733 into a reasonable framework can increase confusion and uncertainty in climate change research
734 (Wu et al., 2022). Therefore, it is essential to introduce a structured framework such as MCDA
735 to provide a single integrated result.

736

737 **4.2 Uncertainties of model and ensemble prediction in bias correction methods**

738 In climate modeling, quantifying uncertainty is essential to assess the reliability of bias-
739 corrected precipitation data. This study applied BMA to quantify the uncertainty of three QM
740 methods on a continental basis, addressing both model-specific and ensemble prediction
741 uncertainties. Similar to the findings by Cannon et al. (2015), this analysis demonstrates how
742 different bias correction methods yield varying uncertainty levels based on the underlying
743 climate models. Notably, EQM showed the lowest weight variance across most continents,
744 which means that the inter-model uncertainty for 11 GCMs corrected by EQM is lower than
745 that of the other QM methods. The low uncertainty associated with EQM aligns with previous
746 studies like Themeßl et al. (2012), which found that EQM consistently reduced discrepancies
747 between modeled and observed data across regions. EQM's ability to manage extreme
748 precipitation and anomalous values based on observed distributions contributes to its reliability,
749 a feature also emphasized by Gudmundsson et al. (2012). On the other hand, DQM showed the
750 highest weight variance across all continents, indicating more significant uncertainty when
751 applied to various GCMs. This uncertainty was particularly pronounced in regions with
752 complex climate conditions, such as Southeast Asia, East Africa, and the Alps in Europe. These
753 results align with Berg et al. (2022), who highlighted DQM's limitations in capturing long-term
754 climate trends and extreme events. The higher uncertainty associated with DQM suggests that,
755 while its detrending process is effective in correcting the mean, it may struggle in regions
756 dominated by nonlinear climate patterns, as it does not sufficiently account for all quantiles in
757 the distribution, particularly extremes, as noted by Cannon et al. (2015). QDM, though showing
758 lower weight variance than DQM, still demonstrated higher uncertainty than EQM in regions
759 with diverse climate characteristics. These results are consistent with the study of Tong et al.
760 (2021), suggesting that QDM performs better under moderate precipitation scenarios. However,
761 the uncertainty may increase under highly variable or extreme weather conditions. Furthermore,
762 this study extended the uncertainty analysis to ensemble predictions, calculating the standard
763 deviation of daily precipitation for each continent using BMA. The EQM-based ensemble
764 consistently exhibited low standard deviations across all continents, indicating that EQM offers

765 the most stable and reliable precipitation predictions. This finding echoes the conclusions
766 drawn by Teng et al. (2015), where EQM provided more accurate and less uncertain projections.
767 In contrast, DQM presented the most significant prediction uncertainty, reinforcing the need
768 for caution when applying DQM in studies that require high-confidence data. These results
769 emphasize the importance of weighing performance and uncertainty when choosing a suitable
770 bias correction method. EQM's consistent performance in reducing uncertainty across model-
771 specific and ensemble forecasts highlights its robustness as a preferred choice for climate
772 research. However, the substantial uncertainty associated with DQM suggests that its use
773 should be limited to regions where its detrending process can be beneficial. Overall, these
774 findings stress the critical role of uncertainty quantification in climate change impact
775 assessments and underscore the need for selecting bias correction methods based on a
776 comprehensive evaluation of both performance and uncertainty.

777

778 **4.3 Integrated assessment of bias correction methods**

779 This study selected the optimal QM method for each continent based on the CI, which considers
780 uncertainty and performance. The critical point is that uncertainty is decisive when selecting a
781 bias correction method. As shown in Figure 19, the optimal correction method varies depending
782 on the continent, and the selected method also changes depending on the weight. These results
783 suggest that uncertainty still exists, as Berg et al. (2022) pointed out, and that uncertainty must
784 be considered when selecting the optimal method. In other words, even if the QM method has
785 high performance, it is difficult to make a reasonable selection if the uncertainty contained in
786 the method is significant. Overall, EQM showed the highest CI value in all continents, which
787 means that it provides the most balanced results in terms of performance and uncertainty. These
788 results are consistent with previous studies (Lafon et al., 2013; Teutschbein and Seibert, 2012;
789 Teng et al., 2015) that showed high precipitation correction accuracy and excellent
790 performance, especially under complex climate conditions. QDM was evaluated highly in some
791 regions but performed worse than EQM overall. Berg et al. (2022) also pointed out that QDM
792 is superior in general climate conditions but may perform worse in extreme climate situations,
793 suggesting that this may increase the uncertainty of QDM in extreme climates. DQM was
794 evaluated as an unsuitable method in most regions due to low CI values, which is consistent
795 with the limitations of DQM mentioned in Cannon et al. (2015) and Berg et al. (2022). It was
796 confirmed that DQM performs relatively well in dry climates but may perform worse in various

797 climate conditions. In addition, some differences were observed with the results based on
798 TOPSIS. For example, DQM was selected more than QDM in South America, but when the
799 uncertainty weight was applied, QDM was selected more. Conversely, in Oceania, QDM was
800 selected more than DQM, but when the uncertainty weight was increased to 0.7, DQM was
801 selected more. These results are consistent with those of Lafferty and Srivier (2023), showing
802 that when significant uncertainty exists, uncertainty can be greater despite high bias correction
803 performance.

804

805 **5. Conclusion**

806 This study corrected and compared historical daily precipitation from 11 CMIP6 GCMs using
807 three QM methods. Eleven statistical metrics were used to evaluate the precipitation
808 performance corrected by three QM methods, and TOPSIS was applied to select performance-
809 based priorities. BMA was applied to quantify model-specific and ensemble prediction
810 uncertainties. Additionally, suitable QM methods were selected and compared using a CI that
811 integrates TOPSIS performance scores with BMA uncertainty metrics. The conclusions of this
812 study are as follows:

- 813 1. EQM showed the highest overall index across all continents, indicating that it provides
814 the most balanced approach in terms of performance and uncertainty.
- 815 2. DQM effectively reproduced the dry climate in North Africa and parts of Central and
816 Southwest Asia but showed the highest uncertainty across all continents. These results
817 suggest that DQM may lose some long-term trend information, making it less reliable
818 in regions prone to extreme weather events.
- 819 3. QDM performed better in certain regions, such as Southeast Asia, and was selected
820 more often than DQM when uncertainty was given greater weight. QDM may be a
821 promising alternative in areas where uncertainty plays a significant role.
- 822 4. Selecting an appropriate QM is required for high performance, and significant
823 uncertainty can complicate rational decision-making. Therefore, a multifaceted
824 approach considering performance and uncertainty is essential in climate modeling.

825 **In conclusion, EQM has emerged as the preferred method due to its balanced performance, but**
826 **this study emphasizes the importance of regional assessment and careful consideration of**
827 **uncertainty when selecting a QM method. Furthermore, EQM is the most balanced method**
828 **regarding performance and uncertainty and will likely be preferred in future climate modeling**

829 studies. However, there may be more suitable QM methods depending on the region, and a
830 comprehensive evaluation with various weights is needed. Therefore, when establishing
831 climate change response strategies or policy decisions, it is essential to take a multifaceted
832 approach that considers uncertainty together rather than relying on a single indicator or
833 performance alone. It will enable more reliable predictions and better decision-making. Future
834 research should integrate greenhouse gas scenarios to improve the accuracy of climate
835 predictions and provide a more comprehensive understanding of future climate risks.

836

837 **Code and data availability**

838 Codes for benchmarking the xclim of python package are available from
839 <https://doi.org/10.5281/zenodo.10685050> (Bourgault et al., 2024). Furthermore, the CI
840 proposed in this study, along with the TOPSIS and BMA used within it, is available at
841 <https://doi.org/10.5281/zenodo.14351816> (Song, 2024b). The data used in this study are
842 publicly available from multiple sources. CMIP6 General Circulation Models (GCMs) outputs
843 were obtained from the Earth System Grid Federation (ESGF) data portal at [https://esgf-](https://esgf-node.llnl.gov/search/cmip6/)
844 [node.llnl.gov/search/cmip6/](https://esgf-node.llnl.gov/search/cmip6/). Users can select data types such as climate variables, time series,
845 and experiment ID, which can be downloaded as NC files. Furthermore, CMIP6 GCMs output
846 can also be accessed in Eyring et al. (2016) The ERA5 reanalysis dataset used in this study is
847 available through the Copernicus Data Store (CDS) provided by ECMWF
848 ([https://cds.climate.copernicus.eu/cdsapp#!/dataset/reanalysis-era5-single-](https://cds.climate.copernicus.eu/cdsapp#!/dataset/reanalysis-era5-single-levels?tab=overview)
849 [levels?tab=overview](https://cds.climate.copernicus.eu/cdsapp#!/dataset/reanalysis-era5-single-levels?tab=overview)). ERA5 is available at <https://doi.org/10.24381/cds.bd0915c6> (Hersbach
850 et al., 2023). The daily precipitation datasets from CMIP6 GCM and ERA5 used in this study
851 are available at <https://doi.org/10.6084/m9.figshare.27999167.v5> (Song, 2024c).

852

853 **Author contributions**

854 Young Hoon Song: Conceptualization, Methodology, Data curation, Funding acquisition,
855 Visualization, Writing – original draft, Writing – review & editing. Eun Sung Chung: Formal
856 analysis, Funding acquisition, Methodology, Project administration, Supervision, Validation,
857 Writing-review & editing

858

859 **Declaration of Competing Interests**

860 The authors declare that they have no known competing financial interests or personal
861 relationships that could have appeared to influence the work reported in this paper.

862

863 **Acknowledgement**

864 This study was supported by National Research Foundation of Korea (NRF) (RS-2023-
865 00246767_2; 2021R1A2C200569914)

866

867 **Reference**

- 868 1. Abdelmoaty, H.M., and Papalexiou, S.M.: Changes of Extreme Precipitation in
869 CMIP6 Projections: Should We Use Stationary or Nonstationary Models? *J. Clim.*
870 36(9), 2999-3014, <https://doi.org/10.1175/JCLI-D-22-0467.1>, 2023.
- 871 2. Ansari, R., Casanueva, A., Liaqat, M.U., and Grossi, G.: Evaluation of bias
872 correction methods for a multivariate drought index: case study of the Upper Jhelum
873 Basin. *GMD* 16(7), 2055-2076, <https://doi.org/10.5194/gmd-16-2055-2023>, 2023.
- 874 3. Berg P., Bosshard, T., Yang, W., and Zimmermann, K.: MIIdASv0.2.1 – Multi-scale
875 bias AdjuStment. *GMD* 15, 6165-6180, <https://doi.org/10.5194/gmd-15-6165-2022>,
876 2022
- 877 4. Bourgault, P., Huard, D., Smith, T.J., Logan, T., Aoun, A., Lavoie, J., Dupuis, É.,
878 Rondeau-Genesse, G., Alegre, R., Barnes, C., Beaupré Laperrière, A., Biner, S.,
879 Caron, D., Ehbrecht, C., Fyke, J., Keel, T., Labonté, M.P., Lierhammer, L., Low,
880 J.F., Quinn, J., Roy, P., Squire, D., Stephens, Ag., Tanguy, M., Whelan, C., Braun,
881 M., Castro, D.: *xclim: xarray-based climate data analytics (0.48.1)*. Zenodo [Code],
882 <https://doi.org/10.5281/zenodo.10685050>, 2024.
- 883 5. Cannon, A. J., Sobie, S. R., and Murdock, T.Q.: Bias correction of GCM
884 precipitation by quantile mapping: How well do methods preserve changes in
885 quantiles and extremes? *J. Clim.* 28(17), 6938-6959, <https://doi.org/10.1175/JCLI-D-14-00754.1>, 2015.
- 887 6. Cannon, A.J.: Multivariate quantile mapping bias correction: an N-dimensional
888 probability density function transform for climate model simulations of multiple
889 variables. *Clim. Dyn.* 50, 31–49. <https://doi.org/10.1007/s00382-017-3580-6>, 2018.
- 890 7. Chae, S. T., Chung, E. S., and Jiang, J.: Robust siting of permeable pavement in
891 highly urbanized watersheds considering climate change using a combination of

- 892 fuzzy-TOPSIS and the VIKOR method. *Water Resour. Manag.* 36(3), 951–969,
893 <https://doi.org/10.1007/s11269-022-03062-y>, 2022.
- 894 8. Chua, Z.W., Kuleshov, Y., Watkins, A.B., Choy, S., and Sun, C.: A Comparison of
895 Various Correction and Blending Techniques for Creating an Improved Satellite-
896 Gauge Rainfall Dataset over Australia. *Remote Sens.* 14(2), 261,
897 <https://doi.org/10.3390/rs14020261>, 2022.
- 898 9. Chung, E. S., and Kim, Y.J.: Development of fuzzy multi-criteria approach to
899 prioritize locations of treated wastewater use considering climate change scenarios.
900 *JEM* 146, 505–516, <https://doi.org/10.1016/j.jenvman.2014.08.013>, 2014.
- 901 10. Cox, P., and Stephenson, D.: A changing climate for prediction. *Science* 317(5835),
902 207–208, <https://www.science.org/doi/10.1126/science.1145956>, 2007.
- 903 11. Deser, C., Phillips, A., Bourdette, V., and Teng, H.: Uncertainty in climate change
904 projections: the role of internal variability. *Clim. Dyn.* 38, 527–546,
905 <https://doi.org/10.1007/s00382-010-0977-x>, 2012
- 906 12. Déqué, M.: Frequency of precipitation and temperature extremes over France in an
907 anthropogenic scenario: Model results and statistical correction according to
908 observed values. *Glob. Planet. Change.* 57(1-2), 16-26,
909 <https://doi.org/10.1016/j.gloplacha.2006.11.030>, 2007.
- 910 13. Ehret, U., Zehe, E., Wulfmeyer, V., Warrach-Sagi, K., and Liebert, J.: HESS
911 Opinions "Should we apply bias correction to global and regional climate model
912 data?". *HESS* 16(9), 3391-3404, <https://doi.org/10.5194/hess-16-3391-2012>, 2012.
- 913 14. Enayati, M., Bozorg-Haddad, O., Bazrafshan, J., Hejabi, S., and Chu, X.: Bias
914 correction capabilities of quantile mapping methods for rainfall and temperature
915 variables. *Water and Climate change* 12(2), 401-419,
916 <https://doi.org/10.2166/wcc.2020.261>, 2021.
- 917 15. Evin, G., Ribes, A., and Corre, L.: Assessing CMIP6 uncertainties at global warming
918 levels. *Clim Dyn.* <https://doi.org/10.1007/s00382-024-07323-x>, 2024.
- 919 16. Eyring, V., Bony, S., Meehl, G., Senior, C., Stevens, B., Stouffer, R., and Taylor, K.:
920 **Overview of the Coupled Model Intercomparison Project Phase 6 (CMIP6)**
921 **experimental design and organization. *Geoscientific Model Development*, 9(5),**
922 **1937–1958. 2016. <https://doi.org/10.5194/gmd-9-1937-2016>**
- 923 17. Galton, F.: Regression Towards Mediocrity in Hereditary Stature. *The Journal of the*

- 924 Anthropological Institute of Great Britain and Ireland 15, 246-263,
925 <https://doi.org/10.2307/2841583>, 1886.
- 926 18. Giorgi, F., and Mearns, L.O.: Calculation of average, uncertainty range, and
927 reliability of regional climate changes from AOGCM simulations via the “reliability
928 ensemble averaging” (REA) method, *J. Clim.* 15, 1141–1158,
929 [https://doi.org/10.1175/1520-0442\(2002\)015<1141:COAURA>2.0.CO;2](https://doi.org/10.1175/1520-0442(2002)015<1141:COAURA>2.0.CO;2), 2000.
- 930 19. Gupta, H.V., Kling, H., Yilmaz, K.K., and Martinez, G.F.: Decomposition of the
931 mean squared error and NSE performance criteria: Implications for improving
932 hydrological modelling. *J. Hydrol.* 377(1–2), 80–91,
933 <https://doi.org/10.1016/j.jhydrol.2009.08.003>, 2009
- 934 20. Gudmundsson, L., Bremnes, J.B., Haugen, J.E., and Engen-Skaugen, T.: Technical
935 Note: Downscaling RCM precipitation to the station scale using statistical
936 transformations – a comparison of methods. *HESS* 16(9), 3383–3390,
937 <https://doi.org/10.5194/hess-16-3383-2012>, 2012.
- 938 21. Hamed, M.M., Nashwan, M.S., Shahid, S., Wang, X.J., Ismail, T.B., Dewan, A., and
939 Asaduzzaman, M.d: Future Köppen-Geiger climate zones over Southeast Asia using
940 CMIP6 Multimodel Ensemble. *Atmos. Res.* 283(1), 106560,
941 <https://doi.org/10.1016/j.atmosres.2022.106560>, 2023.
- 942 22. Hersbach, H., Bell, B., Berrisford, P., Hirahara, S., Horányi, A., Muñoz-Sabater, J.,
943 Nicolas, J., Peubey, C., Radu, R., Schepers, D., Simmons, A., Soci, C., Abdalla, S.,
944 Abellan, X., Balsamo, G., Bechtold, P., Biavati, G., Bidlot, J., Bonavita, M., Chiara,
945 G., Dahlgren, P., Dee, D., Diamantakis, M., Dragani, R., Flemming, J., Forbes, R.,
946 Fuentes, M., Geer, A., Haimberger, L., Healy, S., Hogan, R. J., Hólm, E., Janisková,
947 M., Keeley, S., Laloyaux, P., Lopez, P., Lupu, C., Radnoti, G., Rosnay, P., Rozum,
948 I., Vamborg, F., Villaume, S., and Thépaut, J.: The ERA5 global reanalysis, *Q. J.*
949 *Roy. Meteor. Soc.*, 146, 1999–2049, <https://doi.org/10.1002/qj.3803>, 2020.
- 950 23. Hersbach, H., Bell, B., Berrisford, P., Biavati, G., Horányi, A., Muñoz Sabater, J.,
951 Nicolas, J., Peubey, C., Radu, R., Rozum, I., Schepers, D., Simmons, A., Soci, C.,
952 Dee, D., and Thépaut, J.-N.: ERA5 hourly data on pressure levels from 1940 to
953 present, Copernicus Climate Change Service (C3S) Climate Data Store (CDS),
954 <https://doi.org/10.24381/cds.bd0915c6>, 2023.
- 955 24. Homsí, R., Shiru, M. S., Shahid, S., Ismail, T., Harun, S. B., Al-Ansari, N., and

- 956 Yaseen, Z.M: Precipitation projection using a CMIP5 GCM ensemble model: a
957 regional investigation of Syria. *Eng. Appl. Comput. Fluid Mech.* 14(1), 90–106,
958 <https://doi.org/10.1080/19942060.2019.1683076>, 2019.
- 959 25. Hoeting J.A., Madigan D., Raftery A.E., and Volinsky C.T.: Bayesian model
960 averaging: A tutorial (with discussion). *Stat. Sci.* 214, 382-417,
961 <https://doi.org/10.1214/ss/1009212519>, 1999.
- 962 26. Hosking, J.R.M., Wallis, J.R., and Wood, E.F.: Estimation of the generalized
963 extreme value distribution by the method of probability weighted moments.
964 *Technometrics* 27, 251–261, <https://doi.org/10.1080/00401706.1985.10488049>,
965 1985.
- 966 27. Hosking, J.R.M.: L-moments: Analysis and estimation of distributions using linear
967 combinations of order statistics. *J. R. Stat.* 52, 105–124,
968 <https://doi.org/10.1111/j.2517-6161.1990.tb01775.x>, 1990.
- 969 28. Hwang, C. L., and Yoon, K.: Multiple attribute decision making: Methods and
970 applications. Springer-Verlag. <https://doi.org/10.1007/978-3-642-48318-9>. 1981.
- 971 29. IPCC: Climate Change 2021: The Physical Science Basis. Contribution of Working
972 Group I to the Sixth Assessment Report of the Intergovernmental Panel on Climate
973 Change, edited by: Masson-Delmotte, V., Zhai, P., Pirani, A., Connors, S. L., Péan,
974 C., Berger, S., Caud, N., Chen, Y., Goldfarb, L., Gomis, M. I., Huang, M., Leitzell,
975 K., Lonnoy, E., Matthews, J. B. R., Maycock, T. K., Waterfield, T., Yelekçi, O., Yu,
976 R., and Zhou, B., Cambridge University Press,
977 <https://doi.org/10.1017/9781009157896>, 2021.
- 978 30. IPCC: Climate Change 2022: Impacts, Adaptation, and Vulnerability. Contribution
979 of Working Group II to the Sixth Assessment Report of the Intergovernmental Panel
980 on Climate Change, edited by: Pörtner, H.-O., Roberts, D. C., Tignor, M.,
981 Poloczanska, E. S., Mintenbeck, K., Alegría, A., Craig, M., Langsdorf, S., Löschke,
982 S., Möller, V., Okem, A., and Rama, B., Cambridge University Press,
983 <https://doi.org/10.1017/9781009325844>, 2022.
- 984 31. Ishizaki, N.N., Shiogama, H., Hanasaki, N., Takahashi, K., and Nakaegawa, T.:
985 Evaluation of the spatial characteristics of climate scenarios based on statistical and
986 dynamical downscaling for impact assessments in Japan. *Int. J. Climatol.* 43(2),
987 1179-1192, <https://doi.org/10.1002/joc.7903>, 2022.

- 988 32. Jobst, A.M., Kingston, D.G., Cullen, N.J., and Schmid, J.: Intercomparison of
989 different uncertainty sources in hydrological climate change projections for an alpine
990 catchment (upper Clutha River, New Zealand). *HESS* 22, 3125-3142,
991 <https://doi.org/10.5194/hess-22-3125-2018>, 2018.
- 992 33. Lafferty, D.C., and Sriver, R.L.: Downscaling and bias-correction contribute
993 considerable uncertainty to local climate projections in CMIP6. *npj Clim Atmos*
994 *Sci* 6, 158, <https://doi.org/10.1038/s41612-023-00486-0>, 2023.
- 995 34. Lafon, T., Dadson, S., Buys, G., and Prudhomme, C.: Bias correction of daily
996 precipitation simulated by a regional climate model: a comparison of methods. *Int. J.*
997 *Climatol.* 33, 1367-1381, <http://dx.doi.org/10.1002/joc.3518>, 2013.
- 998 35. Lin, J.: Divergence measures based on the Shannon entropy. *IEEE Transactions on*
999 *Information Theory* 37(1), 145–151, <https://doi.org/10.1109/18.61115>, 1991.
- 1000 36. Maraun, D.: Bias correction, quantile mapping, and downscaling: Revisiting the
1001 inflation issue. *J. Clim.* 26(6), 2137-2143, [https://doi.org/10.1175/JCLI-D-12-](https://doi.org/10.1175/JCLI-D-12-00821.1)
1002 [00821.1](https://doi.org/10.1175/JCLI-D-12-00821.1), 2013.
- 1003 37. Nair, M.M.A., Rajesh, N., Sahai, A.K., and Lakshmi Kumar, T.V.: Quantification of
1004 uncertainties in projections of extreme daily precipitation simulated by CMIP6
1005 GCMs over homogeneous regions of India. *Int. J. Climatol.* 43(15), 7365-7380,
1006 <https://doi.org/10.1002/joc.8269>, 2023.
- 1007 38. Nash, J.E., and Sutcliffe, J.V.: River flow forecasting through conceptual models part
1008 I—A discussion of principles. *J. Hydrol.* 10, 282–290, [https://doi.org/10.1016/0022-](https://doi.org/10.1016/0022-1694(70)90255-6)
1009 [1694\(70\)90255-6](https://doi.org/10.1016/0022-1694(70)90255-6)Return to ref 1970 in article, 1970.
- 1010 39. Pathak, R., Dasari, H.P., Ashok, K., and Hoteit, I., Effects of multi-observations
1011 uncertainty and models similarity on climate change projections. *npj clim. atmos. sci.*
1012 6, 144, <https://doi.org/10.1038/s41612-023-00473-5>, 2023.
- 1013 40. Petrova, I.Y., Miralles, D.G., Brient, F., Donat, M.G., Min, S.K., Kim, Y.H., and
1014 Bador, M.: Observation-constrained projections reveal longer-than-expected dry
1015 spells. *Nature* 633, 594–600, <https://doi.org/10.1038/s41586-024-07887-y>, 2024.
- 1016 41. Piani, C., Weedon, G. P., Best, M., Gomes, S. M., Viterbo, P., Hagemann, S., and
1017 Haerter, J.O.: Statistical bias correction of global simulated daily precipitation and
1018 temperature for the application of hydrological models. *J. Hydrol.* 395(3-4), 199-215,
1019 <https://doi.org/10.1016/j.jhydrol.2010.10.024>, 2010.

- 1020 42. Rahimi, R., Tavakol-Davani, H., and Nasser, M.: An Uncertainty-Based Regional
1021 Comparative Analysis on the Performance of Different Bias Correction Methods in
1022 Statistical Downscaling of Precipitation. *Water Resour. Manag.* 35, 2503–2518,
1023 <https://doi.org/10.1007/s11269-021-02844-0>, 2021.
- 1024 43. Rajulapati, C.R., and Papalexiou, S.M.: Precipitation Bias Correction: A Novel
1025 Semi-parametric Quantile Mapping Method. *Earth Space Sci.* 10(4),
1026 e2023EA002823, <https://doi.org/10.1029/2023EA002823>, 2023.
- 1027 44. Roca, R., Alexander, L. V., Potter, G., Bador, M., Jucá, R., Contractor, S.,
1028 Bosilovich, M. G., and Cloché, S.: FROGS: a daily $1^\circ \times 1^\circ$ gridded precipitation
1029 database of rain gauge, satellite and reanalysis products, *Earth Syst. Sci. Data*, 11,
1030 1017–1035, <https://doi.org/10.5194/essd-11-1017-2019>, 2019.
- 1031 45. Roca, R., and Fiolleau, T.: Extreme precipitation in the tropics is closely associated
1032 with long-lived convective systems. *Commun Earth Environ* 1(18),
1033 <https://doi.org/10.1038/s43247-020-00015-4>, 2020.
- 1034 46. Saranya, M.S., and Vinish, V.N.: Evaluation and selection of CORDEX-SA datasets
1035 and bias correction methods for a hydrological impact study in a humid tropical river
1036 basin, Kerala. *Water Climate Change* 12(8), 3688-3713,
1037 <https://doi.org/10.2166/wcc.2021.139>, 2021.
- 1038 47. Shanmugam, M., Lim, S., Hosan, M.L. Shrestha, S., Babel, M.S., and Viridis, S.G.P.:
1039 Lapse rate-adjusted bias correction for CMIP6 GCM precipitation data: An
1040 application to the Monsoon Asia Region. *Environ Monit Assess.* 196, 49,
1041 <https://doi.org/10.1007/s10661-023-12187-5>, 2024.
- 1042 48. Smitha, P.S., Narasimhan, B., Sudheer K.P., and Annamalai, H.: An improved bias
1043 correction method of daily rainfall data using a sliding window technique for climate
1044 change impact assessment. *J. Hydrol.* 556, 100-118.
1045 <https://doi.org/10.1016/j.jhydrol.2017.11.010>, 2018
- 1046 49. Song, J. Y., and Chung, E.S.: Robustness, uncertainty, and sensitivity analyses of
1047 TOPSIS method to climate change vulnerability: Case of flood damage. *Water*
1048 *Resour. Manag.*, 30(13), 4751–4771, <https://doi.org/10.1007/s11269-016-1451-2>,
1049 2016.
- 1050 50. Song, Y.H., Shahid, S., and Chung, E.S.: Differences in multi-model ensembles of
1051 CMIP5 and CMIP6 projections for future droughts in South Korea. *Int. J. Climatol.*

- 1052 42(5), 2688-2716, <https://doi.org/10.1002/joc.7386>, 2022a.
- 1053 51. Song, Y.H., Chung, E.S., and Shahid, S.: The New Bias Correction Method for Daily
1054 Extremes Precipitation over South Korea using CMIP6 GCMs. *Water Resour.*
1055 *Manag.* 36, 5977–5997, <https://doi.org/10.1007/s11269-022-03338-3>, 2022b.
- 1056 52. Song, Y.H., Chung, E.S., and Shahid, S.: Uncertainties in evapotranspiration
1057 projections associated with estimation methods and CMIP6 GCMs for South Korea.
1058 *Sci. Total Environ.* 825, 153953, <https://doi.org/10.1016/j.scitotenv.2022.153953>,
1059 2023.
- 1060 53. Song, Y.H., Chung, E.S., and Shahid, S.: Global Future Climate Signal by Latitudes
1061 Using CMIP6 GCMs. *Earths Future* 12(3), e2022EF003183,
1062 <https://doi.org/10.1029/2022EF003183>, 2024a.
- 1063 54. Song, Y.H.: *Comprehensive Index and Performance-Related Code, Zenodo [Code]*,
1064 <https://zenodo.org/records/14351816>. 2024b
- 1065 55. Song, Y.H.: *Historical Daily Precipitation Data of CMIP6 GCMs and ERA5,*
1066 *Figshare [Dataset]*, <https://doi.org/10.6084/m9.figshare.27999167.v5>. 2024c
- 1067 56. Switanek, M.B., Troch, P.A., Castro, C.L., Leuprecht, A., Chang, H.I., Mukherjee,
1068 R., and Demaria E.M.C.: Scaled distribution mapping: a bias correction method that
1069 preserves raw climate model projected changes. *HESS* 21(6), 2649-2666,
1070 <https://doi.org/10.5194/hess-21-2649-2017>, 2017.
- 1071 57. Tanimu, B., Bello, A.A.D., Abdullahi, S.A. Ajibike, M.A., Yaseen, Z.M.,
1072 Kamruzzaman, M., Muhammad, M.K.I., and Shahid, S.: Comparison of conventional
1073 and machine learning methods for bias correcting CMIP6 rainfall and temperature in
1074 Nigeria. *Theor. Appl. Climatol.* 155, 4423–4452, [https://doi.org/10.1007/s00704-](https://doi.org/10.1007/s00704-024-04888-9)
1075 [024-04888-9](https://doi.org/10.1007/s00704-024-04888-9), 2024.
- 1076 58. Teutschbein, C., and Seibert, J.: Bias correction of regional climate model
1077 simulations for 575 hydrological climate-change impact studies: Review and
1078 evaluation of different 576 methods. *J. Hydrol.* 16, 12-29,
1079 <http://dx.doi.org/10.1016/j.jhydrol.2012.05.052>, 2012.
- 1080 59. Teng, J., Potter, N. J., Chiew, F. H. S., Zhang, L., Wang, B., Vaze, J., and Evans,
1081 J.P.: 2015. How does bias correction of regional climate model precipitation affect
1082 modelled runoff? *HESS* 19, 711–728, <https://doi.org/10.5194/hess-19-711-2015>,
1083 2015.

- 1084 60. Themeßl, M.J., Gobiet, A., and Heinrich, G.: Empirical-statistical downscaling and
1085 error correction of daily precipitation from regional climate models. *Int. J. Climatol.*
1086 31(10), 1530-1544, <https://doi.org/10.1002/joc.2168>, 2012.
- 1087 61. Tong, Y., Gao, X., Han, Z., Xu, Y., and Giorgi, F.: Bias correction of temperature
1088 and precipitation over China for RCM simulations using the QM and QDM methods.
1089 *Clim. Dyn.* 57, 1425-1443, <https://doi.org/10.1007/s00382-020-05447-4>, 2021.
- 1090 62. Yip, S., Ferro, C.A.T., Stephenson, D.B., and Hawkins, E.: A simple, coherent
1091 framework for partitioning uncertainty in climate predictions. *J. Clim.* 24(17), 4634–
1092 4643, <https://doi.org/10.1175/2011JCLI4085.1>, 2011.
- 1093 63. Woldemeskel, F. M., Sharma, A. Sivakumar, B., and Mehrotra, R.: A framework to
1094 quantify GCM uncertainties for use in impact assessment studies. *J. Clim.* 519,
1095 1453–1465, <https://doi.org/10.1016/j.jhydrol.2014.09.025>, 2014.
- 1096 64. Wood, R.R., Lehner, F., Pendergrass, A.G., Schlunegger, S.: Changes in
1097 precipitation variability across time scales in multiple global climate model large
1098 ensembles. *Environ. Res. Lett.* 16 084022. [https://doi.org/10.1088/1748-](https://doi.org/10.1088/1748-9326/ac10dd)
1099 [9326/ac10dd](https://doi.org/10.1088/1748-9326/ac10dd), 2021.
- 1100 65. Wu, Y., Miao, C., Fan, X., Gou, J., Zhang, Q., and Zheng, H.: Quantifying the
1101 uncertainty sources of future climate projections and narrowing uncertainties with
1102 Bias Correction Techniques. *Earths Future*, 10(11), e2022EF002963, 2022.
- 1103 66. Zhang, S., Zhou, Z., Peng, P., and Xu, C.: A New Framework for Estimating and
1104 Decomposing the Uncertainty of Climate Projections. *J. Clim.* 37(2), 365-384,
1105 <https://doi.org/10.1175/JCLI-D-23-0064.1>, 2024.
- 1106